Harmful Algae 139 (2024) 102724

Contents lists available at ScienceDirect

Harmful Algae

journal homepage: www.elsevier.com/locate/hal

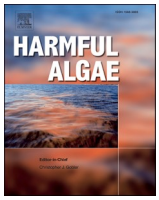

Diversity, toxicity, and distribution of potentially toxic diatoms in Antarctic waters—With description of *Pseudo-nitzschia meridionalis* sp. nov. and *P. glacialis* sp. nov.

Nina Lundholm [a,*], Anneliese L. Christensen [a], Anna K.J. Olesen [a], Bánk Beszteri [b], Sarah Lena Eggers [c], Bernd Krock [d], Andreas Altenburger [e]

[a] Natural History Museum of Denmark, Dept of Biology, University of Copenhagen, Oster Farimagsgade 5, 1353 Copenhagen K, Denmark
[b] Phycology, University of Duisburg-Essen, Universitätsstrasse 2, 45141 Essen, Germany
[c] Alfred Wegener Institut-Helmholtz Zentrum für Polar- und Meeresforschung, Polare Biologische Ozeanographie, Am Handelshafen 12, 27570 Bremerhaven, Germany
[d] Alfred Wegener Institut-Helmholtz Zentrum für Polar- und Meeresforschung, Ökologische Chemie, Am Handelshafen 12, 27570 Bremerhaven, Germany
[e] The Arctic University Museum of Norway, UiT - the Arctic University of Norway, Lars Thørings veg 10, 9006 Tromsø, Norway

ARTICLE INFO

Editor: Vera Trainer

Keywords:
Harmful algae
Southern ocean
Domoic acid
Biodiversity
Toxin

ABSTRACT

Diatoms of the genus *Pseudo-nitzschia*, known for their potential toxicity, are integral to the phytoplankton community of the Southern Ocean, which surrounds Antarctica. Despite their ecological importance, the diversity and toxicity of *Pseudo-nitzschia* in this region remain underexplored. Globally, these diatoms are notorious for forming harmful algal blooms in temperate and tropical waters, causing significant impacts on marine life, ecosystems, and coastal economies. However, detailed information on the diversity, morphology, and toxicity of *Pseudo-nitzschia* species in Antarctic waters is limited, with molecular characterizations of these species being particularly scarce.

During three research expeditions to the Southern Ocean, monoclonal strains of *Pseudo-nitzschia* were isolated and cultivated. Stored samples from a fourth expedition, the Brategg expedition, were used to complete the description of particularly *P. turgidula*. Through electron microscopy and molecular analysis, two novel species were identified—*Pseudo-nitzschia meridionalis* sp. nov. and *Pseudo-nitzschia glacialis* sp. nov.—alongside the previously described species *P. subcurvata, P. turgiduloides*, and *P. turgidula*. Toxin assays revealed no detectable levels of domoic acid in *P. turgiduloides, P. turgidula, P. meridionalis* sp. nov. and *P. glacialis* sp. nov. Conversely, *P. subcurvata* was reported in a related study to produce domoic acid and its isomer, isodomoic acid C.

These findings emphasize the need for comprehensive research on the phytoplankton of Antarctic waters, which is currently a largely uncharted domain. With the looming threat of climate change, understanding the dynamics of potentially harmful algal populations in this region is becoming increasingly critical.

1. Introduction

The Southern Ocean (the Antarctic Ocean) is a unique environment. It comprises about 10 % of the global ocean surface, covering an area of approximately 35 million square kilometers north of the Antarctic coastline (Griffiths, 2010; David and Saucède, 2015). The northern boundary is somewhat dynamic and defined by cold northbound Antarctic water meeting the warmer subtropical waters of the Pacific, Atlantic, and Indian Ocean. The wind-driven Antarctic Circumpolar Current is unrestrained by land and encircles Antarctica between latitudes 45°S and 55°S. This powerful and continuous current is a defining feature of the Southern Ocean, strongly influencing the regional climate and biodiversity (David and Saucède, 2015). The Southern Ocean is known for extreme seasonal fluctuations, from winter, when direct sunlight is entirely absent from 66°S and southwards, to spring, when sunlight initiates an explosive growth of phytoplankton that constitutes the basis of the entire ecosystem's annual cycle (Smith et al., 2007; David and Saucède, 2015; Jabre et al., 2021).

Within the Antarctic phytoplankton community, the average size of primary producers is larger than e.g. in subtropical and tropical regions.

* Corresponding author.
E-mail addresses: nlundholm@snm.ku.dk (N. Lundholm), anneliese.christensen@snm.ku.dk (A.L. Christensen), anna.olesen@snm.ku.dk (A.K.J. Olesen), bank.beszteri@uni-due.de (B. Beszteri), lena.eggers@awi.de (S.L. Eggers), bernd.krock@awi.de (B. Krock), andreas.altenburger@uit.no (A. Altenburger).

https://doi.org/10.1016/j.hal.2024.102724
Received 25 June 2024; Received in revised form 30 August 2024; Accepted 5 September 2024
Available online 12 September 2024

Diatoms are one of the dominating groups (Smith et al., 2007; Armbrust 2009; David and Saucède, 2015) contributing 50–90 % of the biomass in the Southern Ocean in January and December (Arrigo et al., 1999; Alvain et al., 2008; Costa et al., 2020). Together with the haptophyte *Phaeocystis antarctica*, diatoms account for 75–95 % of the primary production, forming the basis of the Antarctic food webs (Fryxell and Kendrick 1988; Smith et al., 2007; Rousseaux and Gregg, 2014). In Antarctic waters, diatoms frequently bloom in the stratified waters adjacent to sea ice floes, where they may account for > 90 % of the phytoplankton community (Andreoli et al., 1995; Garrison et al., 2003). Like some other diatoms, the potentially toxic diatom genus *Pseudo-nitzschia* plays a prominent role in the marine environment, especially in the nutrient-rich waters of the polar regions (Andreoli et al., 1995; Malviya et al., 2016; Mangoni et al., 2017). *Pseudo-nitzschia* H. Peragallo is among the most commonly encountered and dominant diatom genera in Antarctic waters, e.g. contributing 13–70 % of diatom densities in the Weddell Sea and Ross Sea (Fryxell and Kendrick, 1988; Garrison et al., 2003; Almandoz et al., 2008; Saggiomo et al., 2021). Despite the critical role of diatoms in Antarctic ecosystems and their contribution to marine nutrient cycles, there remains a notable gap in our understanding of their taxonomy, diversity, distribution, and ecology in Antarctic waters (Costa et al., 2020; Saggiomo et al., 2021).

Decades ago, *Pseudo-nitzschia* came into the spotlight when it was discovered to form harmful algal blooms (HABs) capable of producing the neurotoxin domoic acid (DA) (Bates et al., 1989). Domoic acid has been detected in a variety of marine organisms across benthic and planktonic food webs ranging from polychaetes (Baustian et al., 2018) and cephalopods (Lopes et al., 2013) to marine mammals (Jensen et al., 2015; McHuron et al., 2013; McCabe et al., 2016). Monitoring efforts have since linked *Pseudo-nitzschia* blooms to unusual mortality events of a wide range of marine mammals (sea otters, seals, sea lions, porpoises, dolphins, toothed and baleen whales) and seabirds (See Lelong et al., 2012, Trainer et al., 2012 and Bates et al., 2018 for references). The presence of DA in all 13 examined marine mammal species from Arctic and subarctic Alaska (Lefebvre et al., 2016) is especially concerning in relation to polar regions. With global warming leading to decreased sea ice and increased light penetration, the conditions for growth of *Pseudo-nitzschia* in both Arctic and Antarctic waters may be enhanced, raising concerns for future polar ecosystems.

The intensified global focus on *Pseudo-nitzschia* has led to an increase in the number of recognized *Pseudo-nitzschia* species, escalating from 20 species in 1994 (Hasle, 1994) to 37 in 2012 (Lelong et al., 2012) and approximately 60 by 2024 (Bates et al., 2018; WoRMS, 2024). Since then, at least four additional species have been identified, though descriptions are pending publication (Lundholm, unpublished). In contrast, the number of described species in the Southern Ocean remained unchanged for decades. This stagnation illustrates the lack of knowledge on the distribution, diversity, and toxicity of *Pseudo-nitzschia* spp. in Antarctic waters, despite their recognized importance to the region's phytoplankton community (Estrada and Delgado, 1990; Kang and Fryxell, 1993).

1.1. Antarctic Pseudo-nitzschia

Presently, seven *Pseudo-nitzschia* species are known from the Antarctic region (Table 1, Scott and Thomas, 2005; Hasle 1964, 1965; Hasle and Medlin 1990; Kang et al., 1993,2001; Ferrario and Licea 2006; Almandoz et al., 2008; Saggiomo et al., 2021). Among these, *P. subcurvata* (Hasle) G.A.Fryxell, *P. prolongatoides* (Hasle) Hasle and *P. turgiduloides* Hasle are endemic to Antarctic waters, while *P. heimii* Manguin, *P. lineola* (Cleve) Hasle, and *P. turgidula* (Hustedt) Hasle are more widely distributed but common in the region (Hasle and Syvertsen, 1997). The seventh species, *P. antarctica,* has only been detected once in the Southern Ocean, and nothing is known about the species beyond the original type description (See Bates et al., 2018). Phylogenetic studies and species delineation within *Pseudo-nitzschia* often utilize the ITS1–5.8S-ITS2 rDNA. However, sequences from Antarctic waters are currently only available for two taxa; one strain of *P. turgiduloides* (Lundholm et al., 2003), and three strains of *P. subcurvata* (Lundholm et al., 2006; Hamsher et al., 2011).

Table 1
Distribution and toxicity of *Pseudo-nitzschia* species recorded in Antarctic waters. nd = no data. Limit of detection was between 1.38×10^{-5} and 2.75×10^{-5} pg cell^{-1} in Olesen et al. (2021), and $3.28\ 10^{-3}$ pg cell^{-1} in Fryxell et al. (1991). Similar specific detection levels were not given in the other publications.

Species	Global Distribution	Toxicity in Antarctica	Toxicity elsewhere
P. antarctica	Antarctic	nd	
***P. glacialis* sp. nov.**	Subantarctic	No: **present study (3 strains)**	nd
P. heimii	From Subarctic to Antarctic	nd	No: Marchetti et al., 2008
P. lineola	Global, except Arctic and Subarctic	No: Kang et al., 1993 (1 strain)	No: Lundholm et al., 2012
***P. meridionalis* sp. nov.**	Antarctic	No: **present study (2 strains)**	
P. prolongatoides	Antarctic	nd	
P. subcurvata	Subantarctic and Antarctic	Yes: Olesen et al., 2021 **(3 strains)** No: Fryxell et al., 1991 (1 strain), Kang et al., 1993 (2 strains), Lundholm et al., 2018 (1 strain), Olesen et al., 2021 (12 strains), **present study (2 strains)**	
P. turgidula	From Subarctic to Antarctic	No: **present study (1 strain)**	No: Marchetti et al., 2008); Yes: Fernandes et al., 2014 (from North Western Atlantic)
P. turgiduloides	Antarctic	No: Kang et al., 1993 (2 strains), **present study (4 strains)**	

The same lack of knowledge exists regarding the toxicity of *Pseudo-nitzschia*. The number of known toxic species is increasing in many regions of the world (Bates et al., 2018) whereas strains from Antarctic waters were first proven toxic in 2021 (Olesen et al., 2021). Prior to this discovery, toxicity tests on seven Antarctic strains, representing *P. lineola, P. subcurvata*, and *P. turgiduloides*; yielded no evidence of toxin production (Table 1). Consequently, four Antarctic species have yet to be examined for domoic acid (DA) production. Among the species tested, *P. heimii* and *P. lineola* have not been found to produce toxins elsewhere in the world (Marchetti et al., 2008; Lundholm et al., 2012). In contrast, *P. turgidula* strains from the Gulf of Maine have tested positive for DA (Fernandes et al., 2014), while strains from the Northeast Pacific were negative for DA (Marchetti et al., 2008).

Recent findings suggest that DA is present in or close to Antarctic waters, and possibly already affects animals in the Southern hemisphere. High levels of DA were detected in fecal samples of southern right whales (*Eubalaena australis*) while feeding on calving grounds at the Argentinian east coast with copepods being the most likely vector of DA (D'Agostino et al., 2017). Furthermore, DA was detected in the water column of the Antarctic Pacific during a large-scale iron fertilizer experiment in 2002 reaching levels up to 220 ng L^{-1} (Silver et al., 2010). Similar DA levels have been linked to animal mortalities off the coast of California (Schnetzer et al., 2007; Scholin et al., 2000).

When comparing with the Arctic, a region with characteristics like the Southern Ocean in terms of temperature, solar radiation and sea ice cover, the finding of DA in all 13 examined marine mammal species from Arctic and subarctic Alaska (Lefebvre et al., 2016) is especially concerning (Lefebvre et al., 2016). Furthermore, Arctic *Pseudo-nitzschia*

species like *P. seriata* (Cleve) H.Peragallo and *P. obtusa* (Hasle) Hasle & Lundholm contain high cellular amounts of DA (Hansen et al., 2011; Harðardóttir et al., 2015; Tammilehto et al., 2012). These findings underscore the urgency to intensify efforts of exploring taxonomy, biodiversity and toxicology of potentially DA-producing *Pseudo-nitzschia* in Antarctic waters. These efforts are essential to understand the potential for harmful algal blooms, and for understanding ecosystem dynamics and the effects of environmental factors.

Utilizing strains of *Pseudo-nitzschia* collected during three Antarctic cruises as well as older field material from Antarctic waters, we conducted an in-depth study of the taxonomy, biodiversity and toxin content of *Pseudo-nitzschia* in Antarctic waters. Here, we revise the present morphological descriptions and describe two new species. Furthermore, we review the present knowledge on diversity, morphology, toxicology, and distribution of Antarctic *Pseudo-nitzschia* species. This will provide a future baseline for expanding our knowledge on these ecologically important phytoplankton species. In our evaluation of the literature regarding the composition of the *Pseudo-nitzschia* community, we considered only descriptions that include identification by electron microscopy (EM) of the species, except for the type descriptions. *Pseudo-nitzschia* species are notoriously difficult to identify. Reliable identification therefore requires either EM or molecular data and in some cases, a combination of both.

2. Materials and methods

Water samples were collected at 10 to 15 m depth during two expeditions to the Southern Ocean (PS103 and PS117) in 2016 and 2018/2019, as well as an expedition to the Ross Sea, Jan.–Feb. 1999. A review of the present diversity of *Pseudo-nitzschia* revealed the presence of seven species some endemic to Antarctic waters others more widespread (Fig. 1, Table 1). A total number of 48 strains were successfully established into monoclonal cultures by isolating single cells or chains (Table S1). From the Southern Ocean expeditions in 2016 and 2018/2019, 24 strains originate from 11 different sample stations between 44.4°S – 69.3°S and 7.5°E – 17.23°W, including a Subantarctic locality as the northernmost station (Fig. 1). Another 24 strains were established from four stations in the Ross Sea, spanning 66.98°S – 75°S and 140°W – 150°W (Table S1). Finally, preserved field samples of the Brategg expedition Dec 1947-Feb 1948 from 53°S – 70°S and 60°W – 174°W were kindly provided by Grethe Rytter Hasle, and used mainly for details on *P. turgidula* (Table S2).

2.1. Morphological analyses

The cultures were studied by light microscopy using an Olympus BX53 microscope with an Olympus DP10 camera (Olympus, Tokyo, Japan), as well as electron microscopy. For the latter, strains were rinsed according to Lundholm et al. (2002), drops of the rinsed material were mounted on carbon-coated grids and left to dry. The grids were inspected in a transmission electron microscope (TEM) (JEOL 1010, Tokyo, Japan). For SEM, a few drops of rinsed material were added to round cover glasses and left to dry. The glasses were glued to metal stubs with double-sided tape, sputter-coated with gold/palladium and examined using a SEM (JEOL JFC 2300HR, Tokyo, Japan). Morphological analyses of the strains included assessments of valve shape and size, along with detailed morphometric characteristics of the valve and girdle.

2.2. Molecular analyses

DNA was extracted from cell pellets using the CTAB method (See Lundholm et al., 2002). For amplification of the ITS1–5.8S-ITS2 region of the nuclear rDNA, the primers ITS1, ITS4 (White et al., 1990) or ITS4Ps (5′-TCCTCCGCTTAATTATATGC-3′) were used. PCR reactions were performed in 25 µl reactions containing 1.5 mM $MgCl_2$, 0,8 mM dNTPs [VWR #733–1363], 0.5 units of polymerase [VWR #733–1301] and 0.4 µM of each primer. The PCR protocol consisted of 36 cycles: 95 °C for 30 s; 55 °C for 30 s; 72 °C for 50 s (initial 2 min at 95 °C, final extension 5 min at 72 °C). The PCR products were sent to Macrogen (Macrogen Europe, Amsterdam, NL) for purification and bidirectional sequencing. Sequence analysis (trimming, assembly, BLAST) was conducted using Geneious version 2022.1.1.

Sequences of ITS rDNA of *Pseudo-nitzschia* species were retrieved

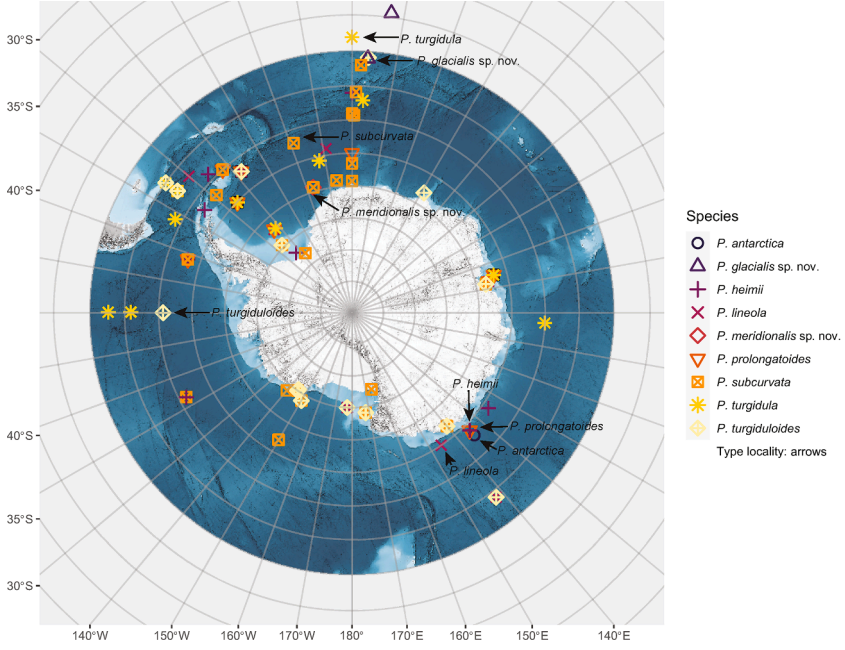

Fig. 1. Map of Antarctic waters with sampling stations as well as records of *Pseudo-nitzschia* species in present and previous studies (Hustedt, 1952, Manguin, 1957, 1960, Hustedt 1958, Hasle 1964, 1965, Fryxell et al., 1991, Kang et al., 1993, 2001, 2003, Lundholm et al., 2003, Ferrario et al., 2004, Riaux-Gobin et al., 2003, Scott and Thomas 2005, Ferrario and Licea, 2006, Almandoz et al., 2008, Rigual-Hernández et al., 2015) based on map from https://www.nature.com/articles/s41597–022–01366–7.

from GenBank and aligned using MAFFT with subsequent alignment masking, as implemented in GUIDANCE2 (Landan and Graur, 2008; Sela et al., 2015). GUIDANCE alignment score was 0.80. The masked alignment (columns below confidence score of 0.93 were removed) was trimmed by hand and included 571 characters. Bayesian Inference was performed with MrBayes 3.2.6 using a GTR + I + Γ model as implemented in Geneious® 2023.2.1 (Biomatters Ltd., Auckland, New Zealand) (Huelsenbeck and Ronquist, 2001). The following settings were used: four simultaneous Markov chain Monte Carlo (MCMC) run for 1000,000 generations, sampling every 1000 generations. The first 25 % of trees were discarded as burn in In addition, an RAxML tree was build using Geneious and the same model of DNA evolution (version 8.2.11, start with complete random tree, 1000 bootstrap replicates) (Stamatakis, 2014).

2.3. ITS2 secondary structure comparisons

For ITS2 secondary structures prediction, the ITS2 region was identified in sequences downloaded from GenBank and in sequences generated for this study by using the ITS2 Annotation tool (model: Eukaryotes, Maximum E-value: $E < 1.0$, Minimum size of ITS2: 150 nt) on the Internal Transcribed Spacer 2 Ribosomal RNA Database (The ITS2 Database (uni-wuerzburg.de)). This tool could in most cases only identify the 5.8 motif of the sequences. After deletion of the 5.8S motif and subsequent alignment, a conserved motif of CCC[A/C]CTCA at the beginning of the ITS2 region and T[T/A]TGCTAT at its end could be identified for all sequences considered. ITS2 structures were subsequently predicted for *P. meridionalis* sp. nov., *P. glacialis* sp. nov., *P. arenysensis*, and *P. uniseriata,* using the Model tool on the ITS2 Database (Reuter and Mathews, 2010) and the published structure of *P. qiana* as template (Huang et al., 2019). The predicted structures were written as dot bracket files and visualized with VARNAv3.9 (Darty et al., 2009). Compensatory base changes (CBSs) detection was performed with 4SALE v.1.7 (Seibel et al., 2006), hemi-compensatory base changes (h-CBCs) were observed manually.

2.4. Toxin analyses

A subset of the strains were tested for DA content. For each strain, 45 mL of culture in stationary growth phase were centrifuged at 4 °C, 1811 g for 15 min and the resulting cell pellet stored at −20 °C until further analysis. Cell pellets were extracted with 200 μL of a 1:1 (V/V) mixture of methanol and 0.03 M acetic acid. The extraction procedure followed Krock et al. (2008) and the filtered solution was transferred to HPLC glass vials, sealed and frozen until analysis. DA contents were measured with liquid chromatography coupled to a tandem mass spectrometer (LC-MS-MS) as detailed in Geuer et al. (2020). The detection limit for DA in the samples ranged between 0.9 and 200 fg cell^{-1} (Table S1) depending on available biomass.

3. Results

Through the integration of morphological data from electron microscopy (EM) and molecular analyses of ITS rDNA sequences, 48 *Pseudo-nitzschia* strains were classified into five distinct species. Three of these species are already known from Antarctic waters: *P. subcurvata* (34 strains), *P. turgiduloides* (8 strains) and *P. turgidula* (1 strain). More detailed and precise emended descriptions of these three species are provided below. Two novel species have been identified and are described for the first time: *P. meridionalis* sp. nov. (2 strains) and *P. glacialis* sp. nov. (3 strains) based on differences in morphology, phylogenetic inferences as well as the presence of compensatory base changes (CBC) between the new species and the most closely related taxa. Toxicity of the tested strains are included along with the descriptions below, except for the *P. subcurvata* strains for which toxicity has previously been reported by Olesen et al. (2021).

3.1. *Pseudo-nitzschia subcurvata* (Hasle) G.A.Fryxell, 1993 in Hasle, 1993; Hasle, 1964, Pl. 12 fig. 16

Fig. 2, Table 2.

Holotype. IMBB (Institute of Marine Biology, section for Marine Botany) slide no 10. "Brategg" material (Hasle 1974: 426) stored at Natural History Museum, University of Oslo. Notes: "Brategg" samples (INA). Illustration: Hasle 1964, Pl. 12 fig. 16.

Type locality. Antarctic waters (62°30′S, 19°42′W), January 31, 1957.

Homotypic Synonym. *Nitzschia subcurvata* Hasle 1974

Taxonomic remarks. The detailed description below is based on 34 strains of *P. subcurvata*, encompassing 15 strains from the Southern Ocean and 19 from the Ross Sea (Table S1), in combination with field material from the Brategg expedition. The morphometric data on valve dimensions as well as stria and fibula density were in accordance with the type description of Hasle (1964), and later reports on the taxon (Table 2).

Morphology. The cells appeared in stepped chains with an overlap of 8–16 % of the cell length and with each cell being lanceolate with more or less truncate ends in girdle view (Fig. S1A-B). The valve was narrow (1.4–2.6 μm, Table 2) with a dilated middle part and with long slender rostrate ends, which were slightly enlarged at the tips (Fig. 2A-D). The valve was more or less subcurvate, but always with one margin being straighter than the other more or less convex margin. The fibulae were more or less regularly spaced, 12–20 in 10 μm. No central nodule was present (Fig. 2A-D, F-H). The interstriae, 39–50 in 10 μm, contained one row of hymenate complex poroids with a density of 5–8 in 1 μm (Fig. 2E-F). Each poroid comprised between 3 and 9 sections, with a mean of around 5 sectors (Fig. 2F). Sometimes, some or all poroids were lacking in some or all striae of the valve, with the stria perforation being more or less scattered pores, mainly close to the valvar margins of the striae (Fig. 2G-H). The mantle was 1–2 poroids high. The girdle was composed of three bands, the first band with 49–63 band striae in 10 μm and each stria being 1–2 poroids wide and 1–3 poroids high (Fig. 2I-J). The second band had a similar stria density, but with each stria comprising only 1–2 poroids. The third band was lacking or had scattered poroids. Sometimes a fourth band similar to the third band was present.

Molecular signatures. Genbank accession numbers OP137100, OP137103–4, OP137107, OP137109 of ITS1–5.8S-ITS2 rDNA.

Toxicity. Three of the *P. subcurvata* strains (31–7, 35–12 and M11–04) have previously been described to be toxic, containing domoic acid and isodomoic acid C: 3.09–7.28 10^{-5} pg cell^{-1} and 3.76–8.54 10^{-5} pg cell^{-1}, respectively (Olesen et al., 2021). The remaining 12 strains from the Southern Ocean and strains 2-D and 3–21 from the Ross Sea were all tested negative (Limits of detection were between 0.010 and 1.814 pg cell^{-1}, see Table S1 for details).

Distribution. *Pseudo-nitzschia subcurvata* was observed from stations spanning a broad area of the Southern Ocean (51.99°S - 69.3°S and 2.10°E - 17.23°W), and in the Ross Sea (66.98°S – 75°S and 140°W – 150°W)(Fig. 1), but the species has essentially been recorded from all over Antarctic waters including adjacent to, on and in sea ice (Fig. 1, Table S2; Hasle, 1964).

3.2. *Pseudo-nitzschia turgiduloides* Hasle, 1995

Fig. 3, Table 2

Hasle, 1965, plate 12, figs 9–10

Holotype. IMBB slide No 105, "Brategg" St. 8 material (Hasle, 1995:357). Stored at the Natural History Museum, University of Oslo.

Type locality. Antarctic waters 60°26′S, 90°W, 16. December 1947.

Basionym. *Nitzschia turgiduloides* Hasle, 1965

Homotypic synonym. ***Pseudonitzschia turgiduloides*** **(Hasle)** Hasle, 1993

Heterotypic synonym. ***Pseudo-nitzschia barkleyi*** **var.** ***obtusa***

Table 2
Morphometric data for the three previously recorded *Pseudo-nitzschia* species: *P. subcurvata, P. turgidula* and *P. turgiduloides*. Data are given as min-max, mean ± SD for n number of strains in the present study. For comparison, morphometrics of other studies are given. * indicates type description; ** indicates first detailed description; ' indicates cultured material, nd indicates no data available.

Species	Fibulae in 10 µm	interstriae in 10 µm	Rows of poroids	Poroids in1 µm	Sectors in poroids	Valve length (µm)	Valve width (µm)	Band striae/10 µm	Band structure
P. subcurvata' **(present study: *n* = 11–112)**	**12 - 20** **16.3 ± 2.0**	**39 - 50** **45.2 ± 2.1**	**1**	**5 - 8** **6.5 ± 0.6**	**3 - 9** **5.4 ± 1.1**	**27 - 80** **55.6 ± 11.0**	**1.4 – 2.6** **1.9 ± 0.3**	**49–63** **56.8 ± 3.7**	**1–2 × 1–3**
P. subcurvata (Hasle, 1964)*	12 - 18	44 - 49	1	nd	nd	47 - 90	1.5 - 2.0	nd	nd
P. subcurvata' (Fryxell et al., 1991)	14 - 17	42 - 46	1	nd	nd	46 - 92	2.1 – 2.5	nd	nd
P. subcurvata (Ferrario and Licea 2006; Almandoz et al., 2008)	12 - 22	43 - 55	1	6 - 8	nd	48 - 86	1.3 - 2.0	nd	nd
P. turgiduloides' **(present study: *n* = 16–98)**	**9 – 13** **11.0 ± 1.2**	**16 – 22** **19.1 ± 1.7**	**1 - 2**	**7 – 10** **8.0 ± 0.7**	**None**	**61 - 128** **88.5 ± 25.9**	**1.9 - 2.9** **2.4 ± 0.3**	**None**	**None**
P. turgiduloides (as *P. barkleyi* var. *obtusa*: Manguin 1960)	12	16–20	nd	nd	nd	82	1.5	nd	nd
P. turgiduloides (Hasle 1965)**[x]	10 - 13	17 - 21	1 - 2	8 - 10	nd	63 - 126	1.8 - 2.7	nd	nd
P. turgiduloides (Hasle, 1965)*	10 - 13	17 - 21	1 - 2	nd	nd	63 - 126	1.8 - 2.7	nd	nd
P. turgiduloides (Ferrario et al., 2004; Ferrario and Licea 2006; Almandoz et al., 2008)	10 - 16	17 - 25	1 - 2	7 - 10	nd	81 - 126	1.7 - 2.9	nd	nd
P. turgidula' **(present study: *n* = 8–15)**	**13 - 18** **15.5 ± 1.6**	**23 - 28** **25.7 ± 1.5**	**2**	7 - 8 **7.7 ± 0.5**	**None**	**35 - 77** **51.5 ± 17.9**	**2.5 - 3.5** **2.8 ± 0.4**	**34–40** **36.8 ± 2.8**	**2 × 2–3**
P. turgidula (Hustedt 1958)*	15 - 18	24 - 26	nd	nd	nd	32 - 48	3.0 - 3.5	nd	nd
P. turgidula (Hasle, 1965)**	13 - 18	23 - 28	2	7 - 9	nd	30 - 80	2.5 - 3.5	nd	nd
P. turgidula (Ferrario et al., 2004, Ferrario and Licea 2006; Almandoz et al., 2008)	13 - 18	20 - 28	2	7 - 9	nd	41 - 79	2.3 - 3.5	nd	nd

Manguin, 1960

Taxonomic remarks. The description is based on eight strains identified as *P. turgiduloides*, three from the Southern Ocean and five from the Ross Sea, in combination with the Brategg field material (Table S1). The morphology of the strains was in accordance with the type description by Hasle (1995) (Table 2), and previous technically invalid descriptions of the species (Hasle, 1965, plate 12, figs 9–10, Manguin, 1960).

Morphology: In girdle view, the cells were linear with truncated ends, and the overlap between cells in chains was around 15–23 % of the cell length (Fig. S1 C-D). The valves were almost linear, 1.9–2.9 µm wide (Table 2), very slightly lanceolate, sometimes slightly enlarged in the middle, and with broadly rounded ends (Fig. 3A-C). A central nodule was present, and the fibulae had a density of 9–13 in 10 µm (Fig. 3A-C, G-I). The interstriae were broad and coarsely silicified, 16–22 in 10 µm. The striae comprised 1–2 rows of poroids, sometimes varying within a single stria and sometimes striae in part of the valve all had the same number of rows of poroids (Fig. 3E-I). The poroids were simple, with a hexagonal perforation pattern of the poroid hymen (Fig. 3D). The mantle was very narrow and rarely seen, and with a poroid pattern as the valve. The three girdle bands all completely lacked poroids or any other perforations (Fig. 3J).

Molecular signatures. Genbank accession number OP137111 of ITS1–5.8S-ITS2 rDNA.

Toxicity. Strains 13–50, 13–59, 13–60 and 3–19 were tested negative for toxins (Limit of detection was 175 pg sample^{-1}, but was not calculated per cell).

Distribution. *Pseudo-nitzschia turgiduloides* was identified at station 13 in the Southern Ocean (51°S, 3.59°E), and at station 105 in the Ross Sea (74.98°S, 145.01°W) (Fig. 1). Except for a few cases, it has only been found in Antarctic waters, where it is widely distributed and particularly abundant near or beneath sea ice (Fig. 1, Hasle 1965).

3.3. *Pseudo-nitzschia turgidula (Hustedt) Hasle, 1993*

Fig. 4, Table 3
Simonsen, 1987 vol 3, plate 672, figs 7–15

Holotype. Slide 276/48b in the Hustedt collection. Stored at the Alfred-Wegener Institute.

Type locality. South Atlantic 46°32′S, 0°02′W, 1938–1939 (Simonsen, 1987, vol 1, 452).

Basionym. *Nitzschia turgidula* Hustedt, 1958

Homotypic synonym. *Nitzschia turgidula* Hasle, 1993

Taxonomic remarks. The description is based on a strain (34–6) from the Southern Ocean, in combination with field material from the Brategg expedition, close to the type locality. The morphometric data of the strain agreed with the type description (Hustedt, 1958; Hasle, 1965) and other previous descriptions (Table 2). We excluded the larger cells described as *P. turgidula* in Hasle (1965), as these cells were longer, and had more linear valves with a distinct expansion in the middle - in agreement with a discussion with G.R. Hasle before she died. Additionally, such larger cells were not observed during the analysis of the Brategg material.

Morphology: The cells were symmetric, lanceolate and rhomboid in valve view with rounded ends (Fig. 4A), as presented in the type description in Hustedt (1958) and as the smaller cells in Hasle (1965). In

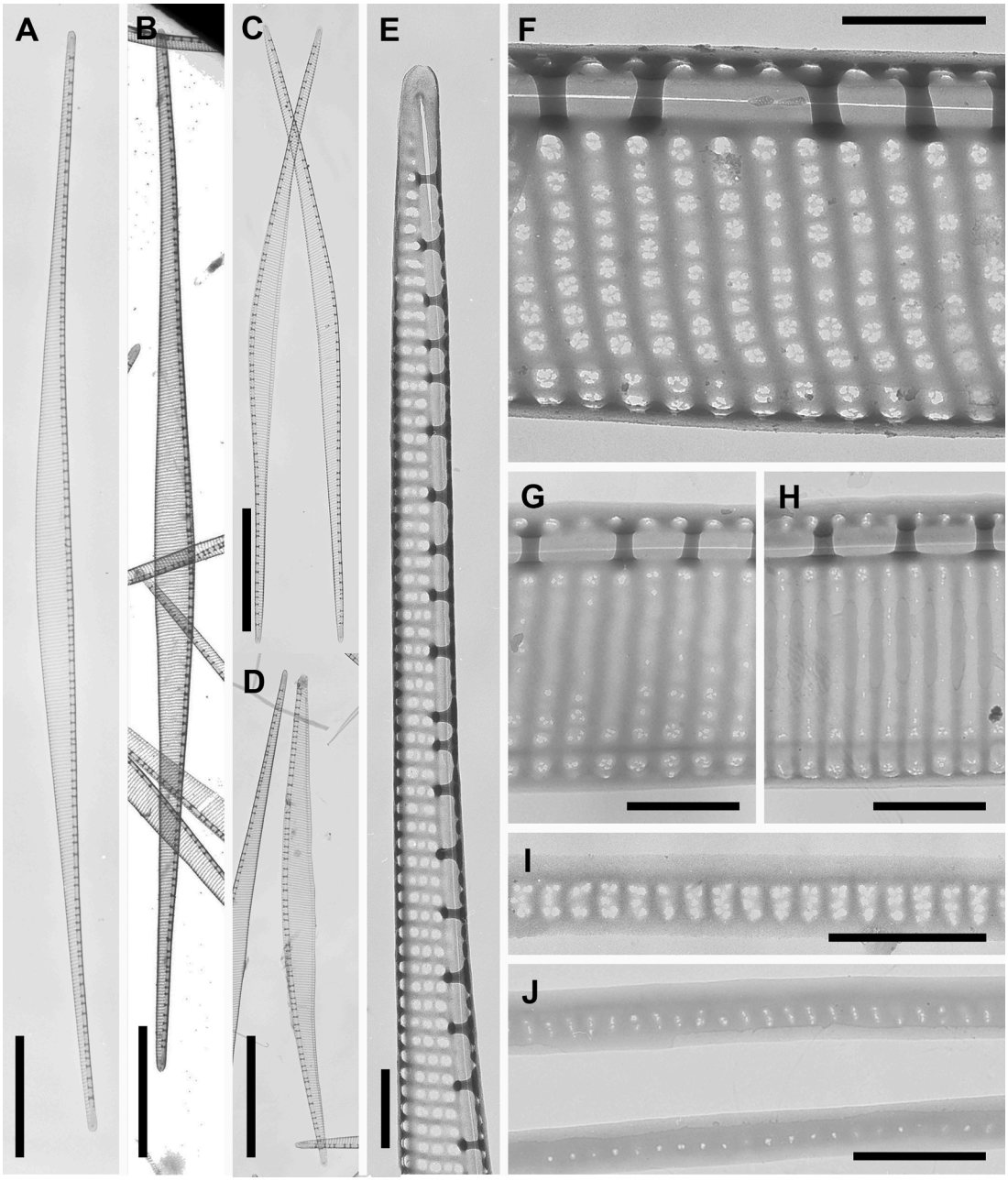

Fig. 2. *Pseudo-nitzschia subcurvata*. TEM. A: Whole cell, strain 1-F. B: Whole cell. Strain 5–19. C: Whole cells, strain 6–1. D: Whole cell strain 6–1. E. Tip of cell, strain 1-F. F: Middle of valve, strain 5–19. G: Middle of valve note reduced poroids, strain 1-F. H: Middle of valve, note almost no poroids, strain 6–5. I: valvocopula, strain 5–19. J: Second and third girdle band, strain 6–5. Scale bars: A-*D* = 10 μm, E-*J* = 1 μm.

girdle view, the sides were almost parallel and slightly lanceolate close to the truncated ends, and with an approximate overlap of 20 %. The valves were 2.5–3.5 μm wide and 35–77 μm long (Table 2). The fibulae were relatively regularly spaced, and separated in the middle of the valve by a central nodule (Fig. 4B-C). The striae contained two rows of small round poroids. The poroid rows were often incomplete towards the middle of the valve, where poroids were mainly present at the edges of each stria (Fig. 4B-C). The size of the poroids varied. Sometimes they were relatively small in two distinct rows separated by a space, whereas at other times, often towards the valve ends, they filled out most of the space between the two interstriae. The mantle structure was similar to the valve and 1–2 poroids high. The first girdle band had band striae at a density of 34–40 in 10 μm, with each band striae being 2 poroids wide and 2–3 poroids high (Fig. 4D-E). The second band had a single row of scattered poroids or band striae with two poroids, and the third band lacked poroids.

Molecular signature. Genbank accession number OP137105 of ITS1–5.8S-ITS2 rDNA.

Distribution. *P. turgidula* was identified in a strain from the Southern Ocean (65.58°S, 12.13°W) and in field material from the area (53°S – 63°S and 60°W – 90°W) (Table S2), and more rarely further south. It thus mainly belongs to the Subantarctic flora. Additionally, it has been recorded in the southern part of the Pacific Ocean, as well as in the Northern Pacific and Atlantic waters (Fernandes et al., 2014; Hasle, 2002).

Toxicity. Strain 34–6 did not contain DA above the limit of detection (Limit of detection was 175 pg sample^{-1}, but was not calculated per cell).

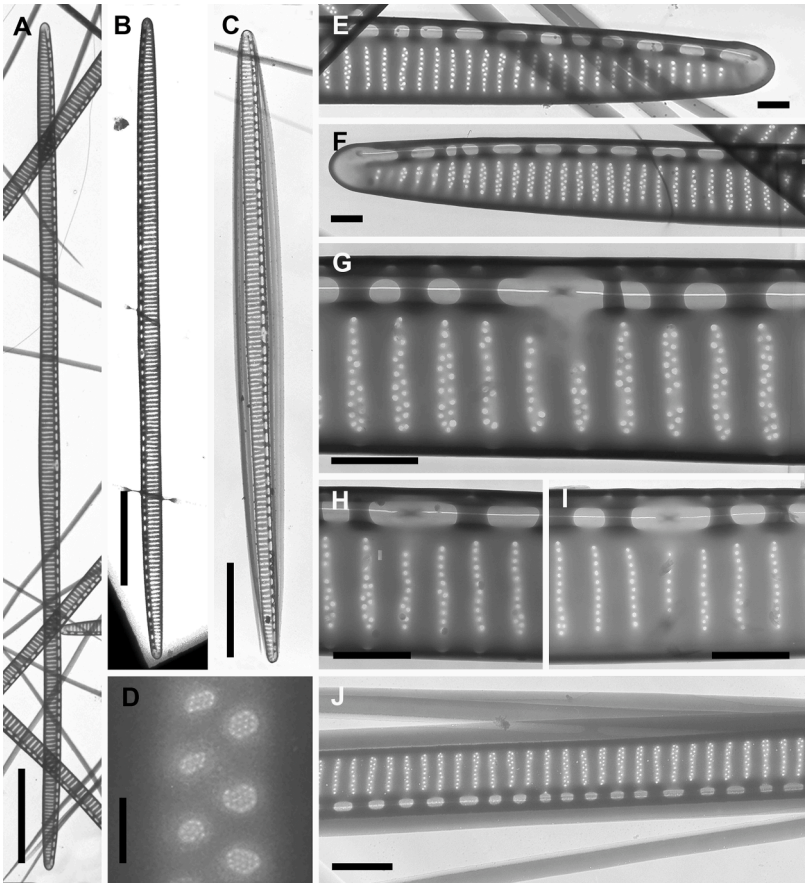

Fig. 3. *Pseudo-nitzschia turgiduloides*. TEM. A: Whole cell, strain 4–16. B: Whole cell, strain 3–19. C: Whole cell with three girdle bands, strain 3–19. D: Hexagonal pattern of poroids, strain 3–19. E: Tip of valve, strain 4–16. F: Other tip of same cell as E, strain 4–16. G: middle of valve with central nodule and two rows of poroids, strain 4–17. H: Middle of valve, one to two rows of poroids, strain 6–1. I: Middle of valve, one row of poroids, strain 4–6. J: valve, valvocopula and other girdle bands, strain 3–19. Scale bars: A-C = 10 μm, *D* = 0.1 μm, E-*I* = 1 μm, *J* = 2 μm.

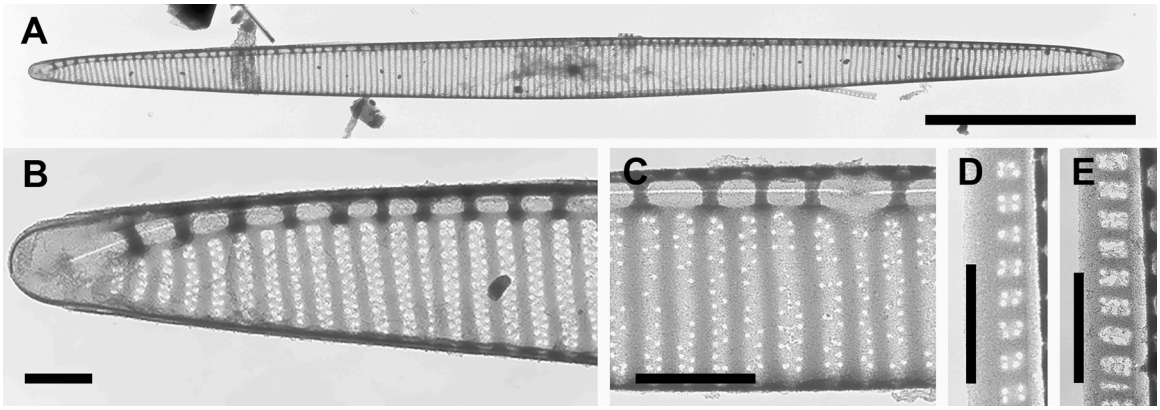

Fig. 4. *Pseudo-nitzschia turgidula*. TEM. A: Whole valve. B: Tip of valve. C: Middle of valve. D: Valvocopula. E: Valvocopula. All field material from Brategg expedition, st. 4 (56°S, 90°W) . Scale bars: *A* = 10 μm, B-*E* = 1 μm.

3.4. Pseudo-nitzschia glacialis sp. nov. Lundholm, Christensen, Olesen

Fig. 5, Table 3

Diagnosis. Overlapping cells in colonies. Cells in valve view lanceolate with rounded tips, 33 – 37 μm long and 3.4 – 3.9 μm wide. Eccentric raphe divided in the middle by central nodule. Fibulae more or less regularly spaced, 14 – 18 in 10 μm, interstriae 28 – 32 in 10 μm. Striae with mainly 2 (sometimes 1–2) rows of simple non-divided poroids, 5 - 9 poroids per μm. Valve mantle structured as valve. Three girdle bands; valvocopula with 38–40 band striae each with 2 × 2–3 poroids, second band with band striae of 2 × 2 poroids or 1 poroid, third band lacking poroids.

Holotype. Fixed material of strain 13–54 deposited at the Natural History Museum of Denmark in Copenhagen, Denmark, registered as CAT99714 illustrated in Fig. 5C, F-H.

Isotype. Material of frustules of strain 13–54 deposited at the Natural History Museum of Denmark in Copenhagen, Denmark, registered as CAT99715.

Table 3
Morphometric data for *P. meridionalis* sp. nov. and *P. glacialis* sp. nov., each compared with morphologically similar taxa. Data are given as min-max, mean ± SD. [1]Lundholm et al., 2012; [2]Dong et al., 2020; [3]Huang et al., 2019; [4]Lundholm et al., 2006; [5]Chen et al., 2021; [6]Teng et al., 2016; [7]Gai et al., 2018; [8]present study.

	Fibulae in 10 μm	Interstriae in 10 μm	Central nodule	Rows of poroids	Poroids in 1 μm	Sectors in poroids	Valve length (μm)	Valve width (μm)	Band striae/ 10 μm	Band structure
***P. meridionalis* sp. nov.** (*n* = 4–104)	**10 – 17** **12.9 ± 1.5**	**25 - 36** **30.7 ± 2.6**	**Yes**	**1 – 2**	**4 – 8** **5.2 ± 1.0**	**1 – 3**	**62 – 77** **67.9 ± 5.1**	**2.1 – 2.8** **2.5 ± 0.2**	**32 – 35** **33.3 ± 1.3**	**1–2 × 2–3;**
P. lineola[1]	11 – 16 13.2 ± 1.0	22 – 31 25.0 ± 2.4	Yes	1 – 2	3 – 7 4.3 ± 0.7	1–2	56 – 112 83.2 ± 5.9	1.8 – 2.8 2.4 ± 0.2	22 – 34 25.4 ± 2.8	2–3 × 2–3
P. uniseriata[2]	14 – 17 15 ± 2	23 – 27 25 ± 2	Yes	1	3 - 4	1–5	82 – 90 86 ± 4	3.1 – 3.6 3.3 ± 0.2	23 – 26 24 ± 2	2 × 2–3
P. qiana[3]	15 – 23 19 ± 1.9	36 – 42 39 ± 1.6	Yes	1	4 – 6 5 ± 1	1 – 3 (4)	49–66 59 ± 6.8	1.3 – 1.5 1.4 ± 0.1	36 - 43	2 × 3–4
P. chiniana[3]	17 – 22 19.3 ± 1.8	30 – 34 32.8 ± 1.3	Yes	1 - 2	4 – 6 5 ± 1	None	42 – 58 49.7 ± 1.5	2.3 – 2.6 2.4 ± 0.1	38 – 40	1–4
P. dolorosa[4]	18 – 22 20.0 ± 1.0	30 – 36 34.5 ± 1.4	Yes	1 - 2	5 – 8 6.6 ± 0.8	None	30 - 59	2.5 – 3.0 2.6 ± 0.2	40 – 44 42.0 ± 1.4	1–4
***P. glacialis* sp. nov.** (*n* = 4–108)	**14 - 18** **16.7 ± 1.2**	**28 – 32** **29.7 ± 1.2**	**Yes**	**2 (1)**	**5 - 9** **6.5 ± 0.9**	**None**	**33 - 37** **34.0 ± 1.4**	**3.4 - 3.9** **3.6 ± 0.2**	**38 – 40** **39.0 ± 0.8**	**2 × 2–3**
P. chiniana[3]	17 – 22 19.3 ± 1.8	30 – 34 32.8 ± 1.3	Yes	1 - 2	4 – 6 5 ± 1	None	42 – 58 49.7 ± 1.5	2.3 – 2.6 2.4 ± 0.1	38 – 40	1–4
P. taiwanensis[5]	15 – 18 15.9 ± 0.9	26 – 28 27.2 ± 0.9	Yes	1	3 – 4 3.8 ± 0.2	0–3, usually 2	101 – 105 103 ± 1.3	2.9 – 3.1 3.0 ± 0.1	33 – 36 34.2 ± 0.9	2 × 2–4
P. bipertita[6]	14 - 20	23 - 28	Yes	2 (1)	5 - 8	1 - 3	65 – 106.6	2.6 – 4.2	31 - 36	2–3 × 3–5
P. bucculenta[7]	16 - 21 18.4 ± 1.2	28 - 35 31.4 ± 1.7	Yes	2 (1)	5 - 7.5 6.7 ± 0.6	None	19 - 31 24.9 – 3.6	2.7 – 3.6 3.0 ± 0.3	38 - 39 38 ± 0.6	2 × 2–4
P. turgidula[8]	13 - 18 15.5 ± 1.6	23 - 28 25.7 ± 1.5	Yes	2	7 - 8 7.7 ± 0.5	None	35 - 77 51.5 ± 17.9	2.5 - 3.5 2.8 ± 0.4	34–40 36.8 ± 2.8	2 × 2–3

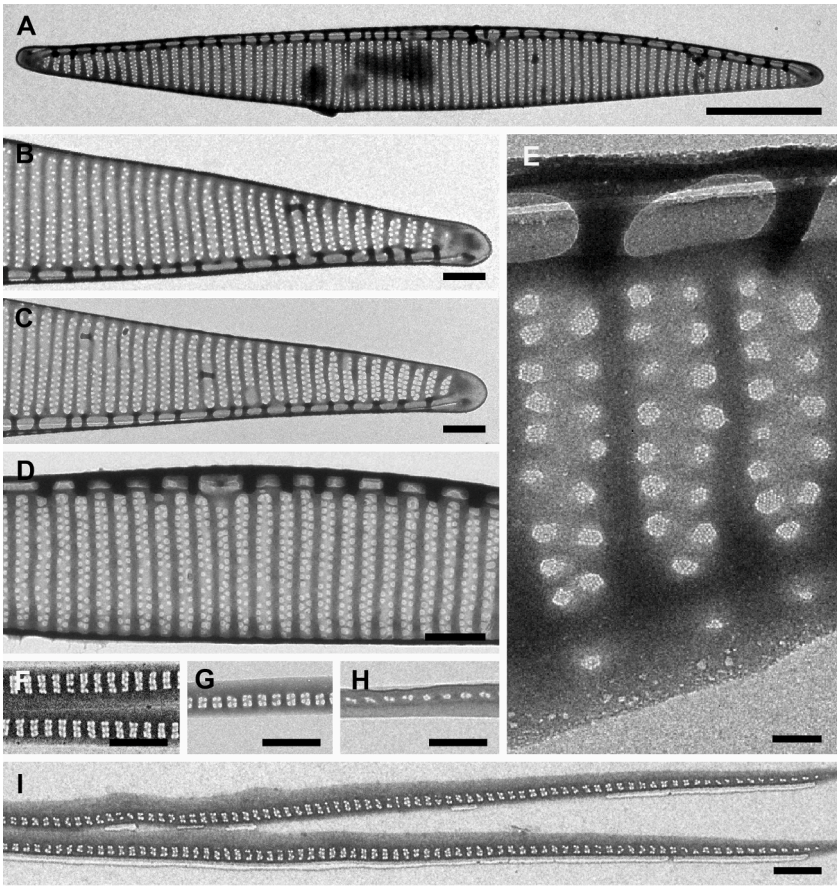

Fig. 5. *Pseudo-nitzschia glacialis*. TEM. A: Whole valve, strain PS117–7–39. B: Tip of valve, one to two rows of poroids, strain PS117–7–39. C: Tip of valve, two rows of poroids, strain PS117–13–54. D: Middle of valve with central nodule, strain PS117–7–39. E: Hexagonal pattern and shape of poroids, PS117–7–39. F: Valvocopula, strain PS117–13–54. G: Valvocopula, strain PS117–13–54. H: second girdle band, strain PS117–13–54. I: Almost complete valvocopula, strain PS117–4–39. Scale bars: *A* = 5 μm, B-D, F-H = 1 μm, *I* = 0.2 μm.

Molecular signature. Nucleotide sequences of rDNA ITS region (ITS1–5.8S-ITS2) of holotype strain 13–54 is deposited at Genbank with accession number OP137106. Additional molecular signatures have been deposited under accession numbers OP137108 and OP137110.

Type locality. The Southern Ocean, 51°S, 3.59°E, strain 13–54 (Fig. 1).

Etymology. The epithet *glacialis* is derived from Latin meaning 'ice', or 'frozen' and refers to the cold waters where the species is found.

Morphology. The cells typically formed stepped chain colonies. They were symmetric and lanceolate in valve view with rounded tips, 33 – 37 μm long and 3.4 – 3.9 μm wide (Table 3, Fig. 5A-C). The eccentric raphe was divided in the middle by a central nodule with a larger interspace between the two central fibulae spanning 3–5 striae (Fig. 5A, D). The fibulae were regularly spaced, 14 – 18 in 10 μm fibulae. The density of the interstriae was 28 – 32 in 10 μm. The striae contained mainly 2, sometimes 1–2, rows of simple non-divided poroids with hexagonal pores and with 5 - 9 poroids in 1 μm (Fig. 5A-E). The size of the poroids varied from small poroids making up two rows separated by a space, to two rows of large poroids taking up most of the stria space (Fig. 5B-E). The valve mantle was structured as the valve and two poroids high (not shown). The girdle comprised three bands, a valvocopula with 38–40 band striae each being 2 poroids wide and 2–3 poroids high (Fig. 5F, I). The second band had band striae of 2 × 2 poroids or only 1 poroid (Fig. 5G-H), while the third band lacked poroids.

Distribution. *P. glacialis* was recorded from two stations in Subantarctic waters (Table S1).

Toxicity. Strains 7–39, 7–41 and 13–54 did not contain DA above the limit of detection (Limit of detection was 175 pg sample^{-1}, but was not calculated per cell).

Secondary structure comparisons of ITS2. The secondary structure analyses of the ITS2 region revealed four compensatory base changes (CBCs) between *P. glacialis* and *P. chiniana* C.X.Huang & Yang Li (Fig. S2). Two consecutive CBCs in helix I with T-A and G-C base pairs in *P. glacialis*, but A-T and T-A, respectively, in *P. chiniana*. One CBC in helix II, with G-C in *P. glacialis*, but T-G in *P. chiniana*. Finally, a fourth CBC was found in helix III with T-A in *P. glacialis*, but C-G in *P. chiniana*. Additionally, ten hemi-CBCs were found scattered in helices I, II and III (See Table S4).

Taxonomic remarks. The description is based on material of the three strains 7–39, 7–41 and 13–54 (Tables 3, S1).

3.5. *Pseudo-nitzschia meridionalis sp. nov. Lundholm, Christensen, Olesen*

Fig. 6, Table 3.

Diagnosis. Overlapping cells in colonies. Cells in valve view symmetric, linear-lanceolate, 62 – 77 μm long, 2.1 – 2.8 μm wide. Eccentric raphe divided in the middle by a central nodule. Fibulae irregularly spaced, 10 – 17 fibulae in 10 μm, 25 – 36 interstriae in 10 μm. Large variation in stria structure: either two clearly defined rows of poroids, only one row of larger poroids, or a transition from one to two rows within the same stria; 4 – 8 poroids in 1 μm. No sectors in poroids present, except with 1 row of larger poroids where poroids may be divided in two parts. Valve mantle structured as valve. Girdle with three bands; valvocopula with 32–35 band striae each with more or less clear 2 × 2–3 poroids, second band with longitudinal row of single poroids or band striae with two poroids. Third band lacking poroids.

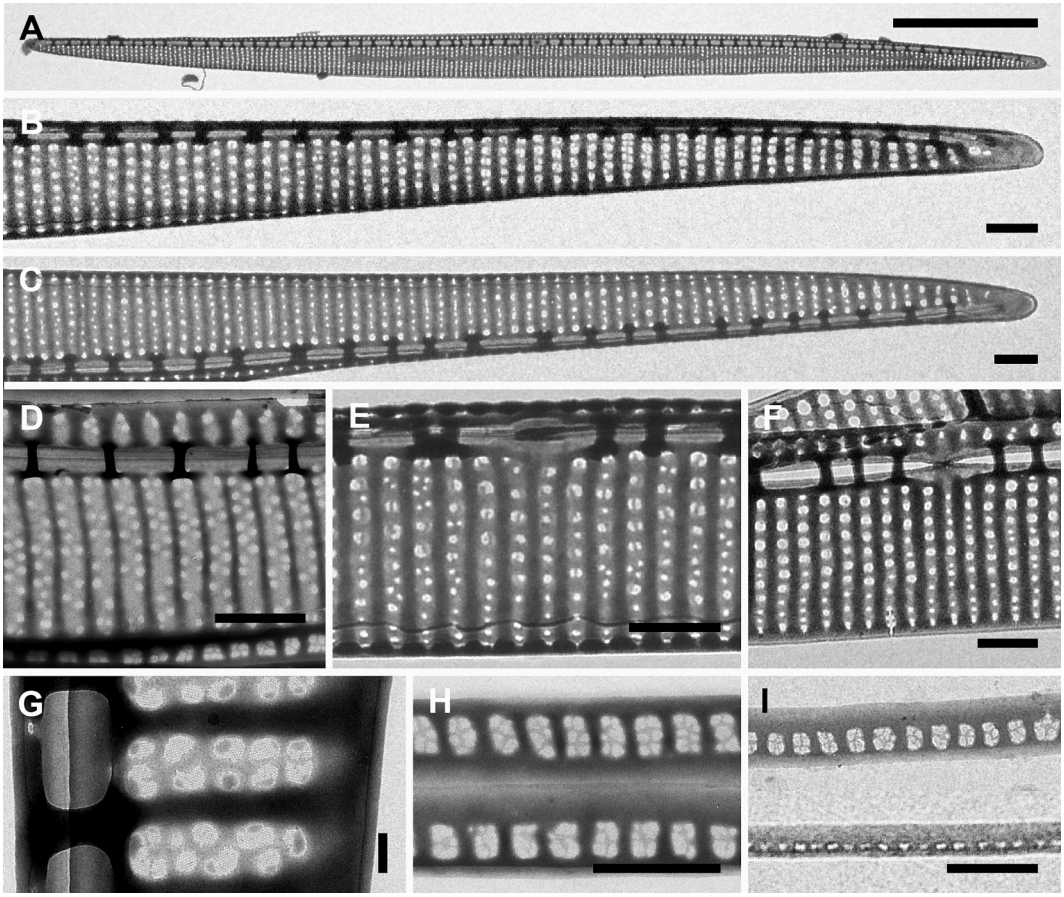

Fig. 6. *Pseudo-nitzschia meridionalis*. TEM, all strain PS117–35–1. A: Whole valve. B: Tip of valve, large poroids. C: Tip of valve, small poroids. D: Part of valve with mantle and two rows of poroids. E: Middle of valve, one to two rows of poroids. F: Middle of valve with central nodule and one row of poroids. G. Hexagonal pattern of poroids. H: Valvocopula. I. Valvocopula and second girdle band. Scale bars: A = 10 μm, B-F, H-I = 1 μm, G = 0.2 μm.

Holotype. Fixed material of strain 35–1 has been deposited at the Natural History Museum of Denmark in Copenhagen, Denmark, registered as CA99716. Illustrated in Fig. 6A-I).

Isotype. Material of rinsed frustules of strain 35–1 deposited at the Natural History Museum of Denmark in Copenhagen, Denmark, registered as CA99717.

Molecular signature. Nucleotide sequence of rDNA ITS region (ITS1–5.8S-ITS2) of strain 35–1 has been deposited in Genbank with accession number OP137102. Another deposited molecular signature is OP137101.

Type locality: Southern Ocean, 69.4°S, 17.18°W

Etymology. The species epithet *meridionalis* (= southern) refers to the Southern Ocean/Southern Hemisphere where the organism was discovered.

Morphology. The cells usually formed stepped chain colonies. In valve view, the cells were linear-lanceolate with relatively pointed tips, 62 – 77 μm long and 2.1 – 2.8 μm wide (Table 3, Fig. 6A-C). The eccentric raphe was divided in the middle by a central nodule spanning 4–5 striae and with a larger space between the two central fibulae (Fig. 6A, E, F). The fibulae were irregularly spaced with 10 – 17 fibulae in 10 μm. The regular interstriae had a density of 25 – 36 interstriae in 10 μm. A huge variation in stria structure was initially very confusing. The striae either comprised two clearly defined rows of poroids (Fig. 6D), only one row of poroids of varying size (Fig. 6F), or a transition from one to two rows of poroids, even within the same stria (Fig. 6E); 4 – 8 poroids in 1 μm. The poroids were often simple but were in some cases divided in 2 (3) sectors in striae with 1 row of larger poroids, as if the two poroids from two rows merged into 1 row (Fig. 6G). The valve mantle was structured as the valve, and two poroids high. The girdle comprised three bands; a valvocopula with 32–35 band striae in 10 μm each with a more or less clear structure being two poroids wide and 2–3 poroids high (Fig. 6H, I), a second band with a longitudinal row of single poroids or band striae with two poroids (Fig. 6I), and a third band lacking poroids.

Toxicity: Strains 35–1 and 35–4 did not contain DA above the limit

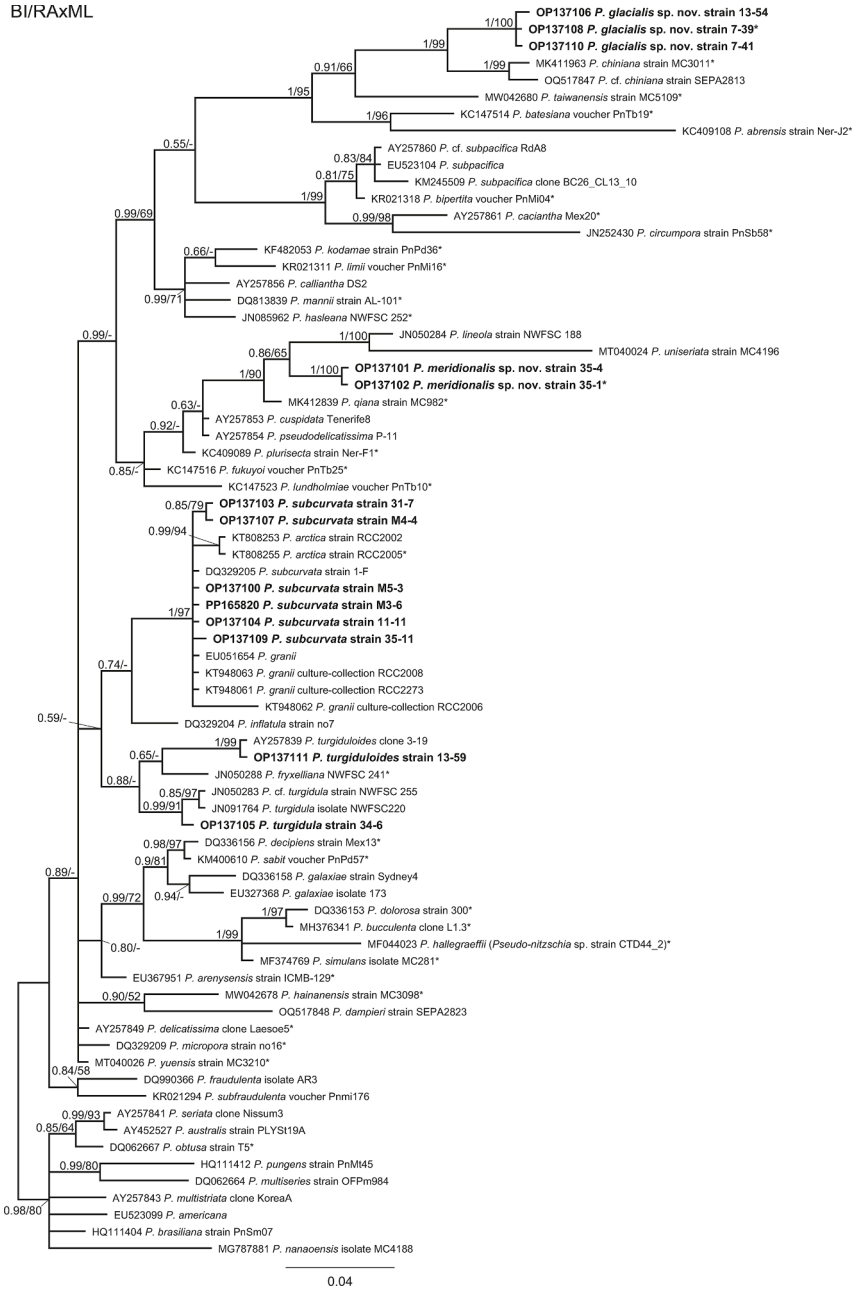

Fig. 7. Phylogenetic BI tree of *Pseudo-nitzschia* spp. interrelations inferred from analyses of ITS1, 5.8S, ITS2 rDNA with support values from BI and RAxML.

of detection (Limit of detection was 175 pg sample^{-1}, but was not calculated per cell).

Distribution. *P. meridionalis* was recorded from a single station (69.3°S, 17.18°W) in the Southern Ocean.

Secondary structure comparisons of ITS2. The structural comparisons of ITS2 revealed two consecutive CBCs in helix III (positions 117–215, 118–214) between *P. meridionalis* and *P. qiana* C.X.Huang & Yang Li, with G-C and T-A in *P. meridionalis* and A-T and G-C, respectively, in *P. qiana* (Fig. S3). A single CBC between *P. meridionalis* (C-G) and *P. lineola* (T-A) was found in helix III (position 116–216). Finally two CBCs in helix III (positions 116–216 and 118–214) differentiated *P. meridionalis* and *P. uniseriata* H.C.Dong & Yang Li, with C-G, T-A in *P.* meridionalis and T-A, G-C, respectively, in *P. uniseriata* (Fig. S3). In addition, four, eight and six hemiCBCs differed between *P. meridionalis* and *P. qiana, P. lineola* and *P. uniseriata,* respectively (Table S5).

Taxonomic remarks. The description provided above pertains to strains 35–1 and 35–4 (Tables 3, S1).

3.6. Phylogenetic inferences

The phylogenetic analyses based on ITS rDNA showed *P. turgiduloides* to cluster with another Antarctic strain of the same species (clone 3–19), and with *P. fryxelliana* Lundholm as sister taxon (Fig. 7). Strains of *P. subcurvata* formed a clade with the morphologically similar *P. granii* (Hasle) Hasle and *P. arctica* Percopo & Sarno. Analyses of a subset of taxa focusing on the *P. subcurvata/P. granii/P. arctica* clade showed the three taxa each forming a monophyletic group, with the Antarctic *P. subcurvata* strains clearly separate from the Subarctic/Arctic *P. granii* with a clade of the Arctic *P. arctica* positioned in between them (Fig. 8). The position of the single *P. turgidula* strain appeared in a clade with other strains of *P. turgidula/P.* cf. *turgidula*, with the Antarctic *P. turgidula* in a separate position. The sister group was a clade comprising *P. turgiduloides* and *P. fryxelliana* (Fig. 7).

The newly described species, *P. meridionalis* and *P. glacialis,* each formed a separate well-supported monophyletic clade consisting of their

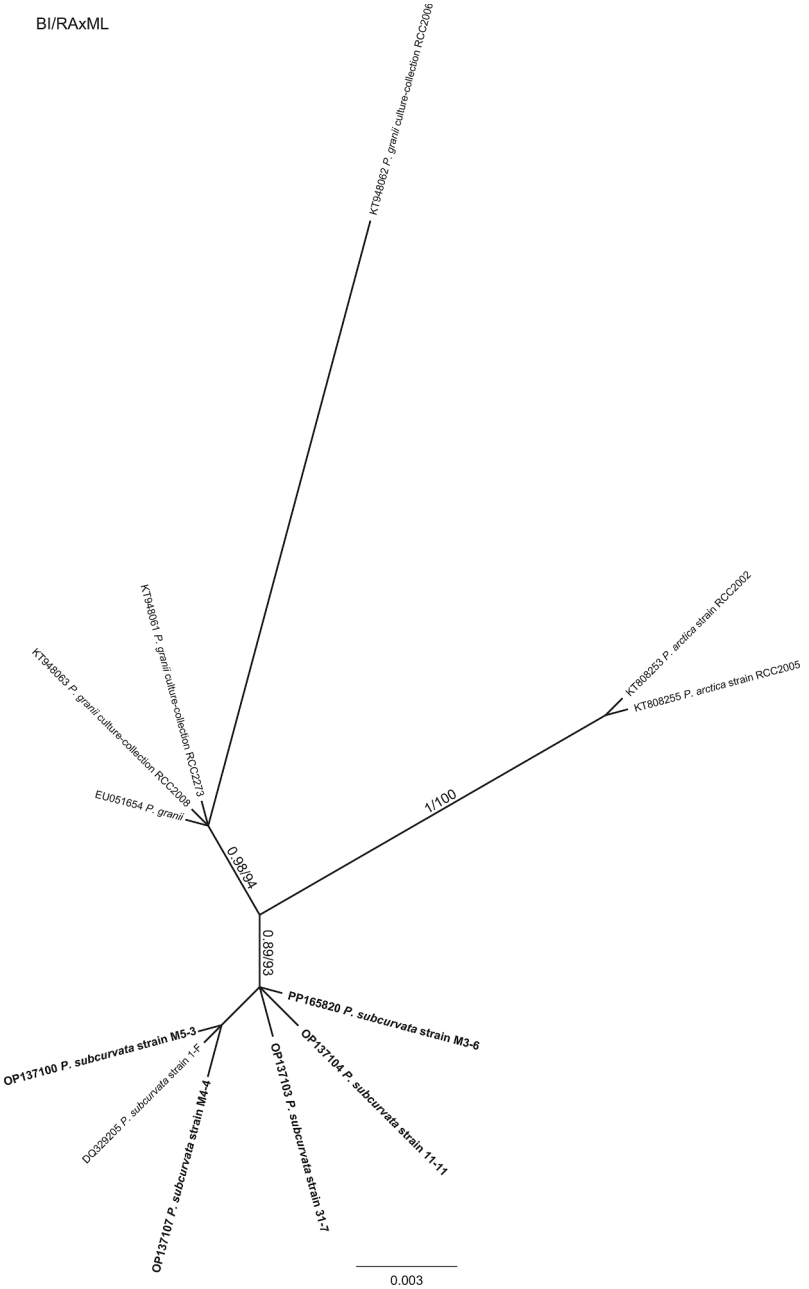

Fig. 8. Phylogenetic BI tree inferred from analyses of ITS1, 5.8S, ITS2 rDNA focusing on P. *subcurvata* and *P. granii* with support values from BI and RAxML.

Table 4
Compilation of morphological data for each listed Antarctic *Pseudo-nitzschia* species, given as min-max and mean ± SD. Data based on references indicated by superscript numbers after species name, except for min-max which is based on present study. [1]Manguin 1960, [2]present study, [3]Manguin, 1957, [4]Hasle 1965, [5]Cleve, 1897, [6]Lundholm et al., 2012, [7]Manguin 1960, [8]Hasle 1964, [9]Lundholm unpubl., [10]Fryxell et al., 1991, [11]Ferrario and Licea 2006, [12]Almandoz et al., 2008, [13]Hustedt 1958, [14]Ferrario et al., 2004, [15]Hasle 1996. nd indicates no data available.

	Valve shape	Fibulae in 10 µm	Striae in 10 µm	Central nodule	Rows of poroids	Poroids in 1µm	Sectors in poroids	Valve length (µm)	Valve width (µm)	Band striae/10 µm	Band structure
P. antarctica[1]	Linear, pointed and sigmoid in ends	14	nd	Yes	nd	nd	nd	100	3 - 4	nd	nd
P. glacialis[2]	Lanceolate, rounded ends	14 - 18	28 – 32	Yes	2 (1)	5 - 9	None	33 - 37	3.4 - 3.9	38 – 40	2 × 2–3
		16.7 ± 1.2	29.7 ± 1.2			6.5 ± 0.9		34.0 ± 1.4	3.6 ± 0.2	39.0 ± 0.8	
P. heimii[3,4,11,12,14]	Linear-lanceolate, ± asymmetrical, obtuse ends	11 - 18	19 - 26	Yes	1 - 2	5 - 8	No	67 - 120	4.0 – 5.7	nd	nd
P. lineola[4–6,11,12,14]	Linear-lanceolate	11 - 18	20 - 31	Yes	1 - 2	3 - 7	No	41 - 125	1.8 – 2.8	22 - 34	2–3 × 2–3
P. meridionalis[2]	Linear-lanceolate	10 – 17	25 - 36	Yes	1 – 2	4 – 8	1 - 3	62 – 77	2.1 – 2.8	32 – 35	1–2 × 2–3;
		12.9 ± 1.5	30.7 ± 2.6			5.2 ± 1.0		68 ± 5	2.5 ± 0.2	33.3 ± 1.3	
P. prolagotoides[4,7,12]	Spindle-shaped, elongated rostrate ends	15 - 21	29 - 35	Yes	2 - 3	8 – 13	nd	20 - 85	0.5 – 2.6	nd	nd
P. subcurvata[2,8–12]	Spindle-shaped, elongated rostrate ends	12 – 22	39 – 55	No	1	5 – 8	3 - 9	27 – 92	1.3 – 2.6	48–86	1–2 × 1–3
		16.3 ± 2.0	45.2 ± 2.1			6.5 ± 0.6		55 ± 11	1.9 ± 0.3	56.8 ± 3.7	
P. turgidula[2,4,11–14]	Linear-lanceolate, rounded ends, expanded in middle	13 – 18	20 – 28	Yes	2	7 – 9	No	30 – 80	2.3 - 3.5	34–40	2 × 2–3
		15.5 ± 1.6	25.7 ± 1.5			7.7 ± 0.5		51 ± 18	2.8 ± 0.4	36.8 ± 2.8	
P. turgiduloides[2,4,7,11,12,14,15]	Linear, rounded ends	9 – 16	16 – 25	Yes	1 - 2	7 – 10	No	61 – 128	1.5 - 2.9	none	none
		11.0 ± 1.2	19.1 ± 1.7			8.0 ± 0.7		89 ± 26	2.4 ± 0.3		

respective strains. The taxon closest to *P. glacialis* was *P. chiniana*, and together they formed a clade with *P. taiwanensis* X.M.Chen & Yang Li as sister taxon. Whereas *P. meridionalis* was found in a clade with *P. uniseriata* and *P. lineola* forming a sister clade and with *P. qiana* in a basal position relative to these three taxa.

4. Discussion

Previous research has documented the presence of six different *Pseudo-nitzschia* species in the Southern Ocean, namely *P. subcurvata, P. turgiduloides, P. prolongatoides, P. lineola, P. turgidula* and *P. heimii* (Almandoz et al., 2008; Hasle and Medlin 1990; Kang and Fryxell, 1993; Kang et al., 2001; Cremer et al., 2003; Scott and Thomas, 2005; Saggiomo et al., 2021). An additional species, *P. antarctica,* was described by Maguin in 1960 but has not been observed since its original description (Manguin, 1960). We found three of the six species in the sample area: *P. subcurvata, P. turgiduloides* and *P. turgidula*. Furthermore, two new species, *P. meridionalis* sp. nov. and *P. glacialis* sp. nov., were identified based on a combination of morphological and molecular analyses, differentiating them from previously described species. The species *P. antarctica* remains elusive, with no molecular or electron microscopic information available. The type description, and the only record, of *P. antarctica*, describes it as having linear valves with sigmoidal and rounded ends, a width of 3–4 µm, and with a central nodule present (Manguin, 1960). It was noted to have 14 fibulae in 10 µm, and the interstriae were invisible under light microscopy, indicating a density greater than 25 per 10 µm. A valve width of >3 µm and the sigmoid ends of the valves clearly differentiates *P. antarctica* Manguin from *P. meridionalis.* Additionally, the valve shape differentiates *P. glacialis* from *P. antarctica*, as *P. glacialis* has symmetric and lanceolate valves, whereas *P. antarctica* has linear and slightly sigmoidal valves. It is therefore unlikely that any of the two herein newly described species are *P. antarctica.*

4.1. *Pseudo-nitzschia glacialis sp. nov and comparison with similar species*

Pseudo-nitzschia glacialis differs from most *Pseudo-nitzschia* species by a unique combination of morphological characters: the presence of a central nodule, two rows of poroids, and a valve width of approximately 3–4 µm. While most *Pseudo-nitzschia* species with a central nodule and two poroid rows tend to have a narrower valve width, there are exceptions such as *P. bipertita* S.T.Teng, H.C.Lim & C.P.Leaw (Teng et al., 2016), *P. bucculenta* Gai, Hedemand, Lundholm & Moestrup (Gai et al., 2018) and *P. turgidula* (Hasle 1965). However, this combination of morphological characters is only informative for identification, rather than for making evolutionary inferences, as these species are not closely related according to the phylogenetic analysis (Fig. 7). The two latter species differ from *P. glacialis* by having a smaller valve width (Table 4). In addition, *P. turgidula* has a lower density of interstriae (23–28 as opposed to 28–30 in *P. glacialis*). The differences between *P. bipertita* and *P. glacialis* are poroids divided into 1–3 sectors in *P. bipertita* whereas *P. glacialis* has simple poroids, and longer cells, as well as a lower density of band striae in *P. bipertita* (Table 4). The phylogenetically closest related taxa, *P. chiniana* and *P. taiwanensis*, mainly differ from *P. glacialis* by having a narrower valve width, fewer rows of poroids, and either 1–2 or 2 rows of poroids, respectively (Huang et al., 2019). In addition, *P. chiniana* differs by having a higher density of fibulae, and *P. taiwanensis* differs by having a lower density of interstriae (Table 4). Considering the known distribution of these species, only *P. turgidula* has been recorded in cold polar waters. The other species have so far only been found in temperate (*P. bucculenta*) (Gai et al., 2018; von Dassow et al., 2023) or subtropical-tropical waters (*P. bipertita, P. chiniana* and *P. taiwanensis*) (Teng et al., 2016; Huang et al., 2019; Dong et al., 2020).

4.2. *Pseudo-nitzschia meridionalis sp. nov and comparison with similar species*

The morphology of the valves of *P. meridionalis* was quite variable, and the strains were at first thought to belong to two different species. The structure of the striae varied from two rows of simple poroids to one row of poroids comprising 1–3 sectors in the poroids. Both strains showed, however, the same variation, and we realized that within a single valve the same variation in stria structure can be present (Fig. 6E); thus a species encompassing a large variation of the striae structure. A similar variable stria structure has been documented in *P. lineola* (Lundholm et al., 2012; Fig. 3) and *P. uniseriata* (Dong et al., 2020; Fig. 5) both of which are phylogenetically close to *P. meridionalis*. The more distantly related species *P. dolorosa* (Lundholm et al., 2006; Fig. 2) and *P. chiniana* (Huang et al., 2019; Fig. 2) also exhibit a variable stria structure. The presence of this morphological trait in both closely related and more distantly related species within the phylogenetic tree suggests that the genus *Pseudo-nitzschia* possesses a limited number of morphological characters, which exhibit a high degree of variability. This variability in inherent character states makes the morphological identification of *Pseudo-nitzschia* species particularly challenging.

Among the species that *P. meridionalis* is evolutionary and morphologically most closely related to is *P. lineola* where the main difference is a smaller density of interstriae and band striae in *P. lineola* (Table 4) (Lundholm et al., 2012). Otherwise, the two taxa are very similar, but form distinctly separate clades in the phylogenetic analyses. The other closely related species, *P. qiana* and *P. uniseriata*, exhibit several differences from *P. meridionalis,* including the densities of interstriae and band striae, valve width, and in the case of *P. qiana,* the density of fibulae (Table 4). Differences between *P. meridionalis* and two other species known for having a variable number of poroids rows, *P. chiniana* and *P. dolorosa,* are apparent in the densities of fibulae and band striae (Table 4). Other species that *P. meridionalis* can be confused with are *P. kodamae* S.T.Teng, H.C.Lim, C.P.Leaw & P.T.Lim (Teng et al., 2014), which has one row of poroids, but sometimes a tendency to two rows. *P. kodamae* is differentiated by having poroids with 2–4 (5) sectors and a slightly lower density of interstriae (Teng et al., 2014). In terms of distribution *P. lineola* is the only one among these closely related or morphologically similar species that has been found in polar waters (Lundholm et al., 2012). *P. dolorosa* has been recorded in cold-warm temperate waters (Lundholm et al., 2006), while the other species (*P. chiniana, P. qiana* and *P. uniseriata*) have only been documented in subtropical waters (Huang et al., 2019; Dong et al., 2020).

4.3. *Pseudo-nitzschia distribution in Antarctica*

The distribution patterns of *Pseudo-nitzschia* species in Antarctic waters reveal ecological preferences and potential temperature tolerances among different species. The discovery of two new *Pseudo-nitzschia* species in the Southern Ocean suggests that the region's diatom diversity is larger than hitherto considered. The new ***P. meridionalis*** was discovered only from station 35 (Fig. 1, Table S1), indicating, based on this very restricted information, that it is adapted to cold-water conditions. In contrast, ***P. glacialis*** was found at two different stations: one in the northern part of the Southern Ocean and, the other near the Antarctic Convergence zone (Fig. 1, Table S1). This distribution suggests that *P. glacialis* may have a broader range, extending beyond just Antarctic waters, and probably more widespread in the Southern Ocean.

P. turgidula and *P. heimii* are predominantly found in the northernmost regions of the Antarctic, which are warmest and farthest from the sea ice, and not in the coldest, most southern waters (Fig. 1). This distribution supports findings from previous studies (Hasle, 1965; Almandoz et al., 2008). *P. glacialis* is likely part of this flora that prefers slightly warmer Antarctic waters. Conversely, other species like *P. subcurvata, P. turgiduloides, P. prolongatoides* and *P. lineola* have been found throughout Antarctic waters, indicating a broader ecological range and possibly a higher tolerance for colder conditions. It is also evident that *P. turgiduloides* and *P. subcurvata* are the most frequently recorded species. The present, as well as several studies found *P. subcurvata* and *P. turgiduloides* to be the most abundant species, often found in high densities (Hasle 1965; Ferrario and Licea, 2006; Almandoz et al., 2008). The species *P. subcurvata, P. turgiduloides, P. prolongatoides* and *P. lineola* have been found in ice, whereas *P. turgidula* and *P. heimii* have not (Garrison et al., 1987; Hegseth and Von Quillfeldt, 2002), aligning with their occurrence in slightly warmer waters.

Pseudo-nitzschia subcurvata stands out as one of the most prevalent species in Antarctic waters, particularly in the southernmost regions (Fig 1, Table S3; Garrison et al., 2003). The geographical distribution of *P. subcurvata* supports the idea that *P. subcurvata* is an endemic Antarctic species (Almandoz et al., 2008; Hasle and Syvertsen, 1997), although it has been recorded in and north of the Polar front in the Drake Passage (Ferrario and Licea, 2006). It has been shown to have optimal growth at 8 °C, supporting it as a real cold-water species.

P. subcurvata is known to reach high densities in various parts of the Southern Ocean, especially in the Ross Sea during spring and summer, where it becomes the most abundant phytoplankton species with recorded densities between 19 and 35.5 $\times$ 10^6 cells L^{-1} (Saggiomo et al., 2021). It often reaches high densities in spring and summer in the surface waters, but may be dominant as early as December in the brine channels of sea ice (Garrison et al., 2003; Thomson et al., 2006). *P. subcurvata* tolerates huge variations in salinity, as it seems to be well adapted to meltwater conditions (Petrou and Ralph, 2011), correlating with its distribution in Antarctic waters where it is found in highest abundance near the ice edge and in shallow water (Almandoz et al., 2008). High abundances of *P. subcurvata* have also been associated with regions characterized by long photoperiods, heavy ice cover and high salinity, similar to *P. turgiduloides* (Almandoz et al., 2008), illustrating the physiological flexibility of the species.

Similar to *P. subcurvata,* ***P. turgiduloides*** is one of the most widely distributed and frequently encountered diatom species in Antarctic waters (Fig 1, Table S3). Both species are considered endemic to Antarctica (Hasle and Syvertsen, 1997). In the Weddell Sea, *P. turgiduloides* has been found throughout the sampling area (60.54° – 67.07°S) and was most abundant in areas with long photoperiods, heavy ice cover, and high salinity conditions that are also favorable for *P. subcurvata* (Almandoz et al., 2008). *P. turgiduloides* may occur in high densities, e.g. in the Ross Sea reaching up to 2.4 $\times$ 10^6 cells L^{-1}. This species is frequently reported in high concentrations (Andreoli et al., 1995; Nuccio et al., 2000; Garrison et al., 2003; Mangoni et al., 2017; Saggiomo et al., 2021)

Compared to the previous two species, ***P. prolongatoides*** is less commonly observed (Fig. 1, Table S3) but is also considered endemic to Antarctic waters (Hasle and Syvertsen, 1997). This species can form dense populations, particularly in spring, where it often co-dominates with *Phaeocystis* in regions with ice (Garrison et al., 2003). In the Weddell Sea, it has been observed in bloom proportions, accounting for >70 % of the diatom cells and reaching concentrations of 7.2 $\times$ 10^5 cells L^{-1}. It is also recognized as one of the five dominating phytoplankton species in the Weddell Sea, both within sea ice and adjacent waters (Garrison et al., 1987; Almandoz et al., 2008). Additionally, its presence has been documented in various other parts of Antarctic waters (Kang and Fryxell, 1993; Kopczynska et al., 1986) suggesting that it is probably a common species in the region (Hasle, 1965).

P. lineola and ***P. turgidula*** are considered cosmopolitan species not exclusive to Antarctic waters (Hasle and Syvertsen 1997). *P. lineola* is well-represented in Antarctic waters (Fig. 1) and has been reported to be abundant in the Ross Sea with concentrations of up to 2.4 $\times$ 10^6 cells L^{-1} (Saggiomo et al., 2021). However, it is typically not as abundant in other parts of the Southern Ocean. *P. turgidula*, on the other hand, tends to be found at lower latitudes within the Antarctic region (Fig. 1).

P. heimii, is not endemic to Antarctica but is frequently found in sub-

Antarctic waters (Hasle and Syvertsen, 1997). This species is primarily observed at lower latitudes, extending as far north as the Weddell Sea, according to Almandoz et al. (2008). While mapping the phytoplankton community during a spring bloom in the Southern Ocean (south of Australia), *P. heimii* was recorded common in an area between 46.9° – 56.9°S and 60.9° - 64.9°S (Kopczynska and Fiala, 2003). Additionally, a spring bloom of *P. heimii* at the Polar Front (56°S-58°S) was documented in 2001 (Ferrario and Licea, 2006). These observations suggest that *P. heimii* is widely distributed in the Southern Ocean and sub-Antarctic waters.

4.4. Potential for toxic blooms of Pseudo-nitzschia in Antarctic waters

Pseudo-nitzschia plays a prominent role in the marine environment, especially in the nutrient-rich waters of the polar regions (Malviya et al., 2016). Numerous studies have documented the high densities of *Pseudo-nitzschia* in Antarctic waters, where it frequently outnumbers other phytoplankton taxa (Hasle 1969; Steyaert 1973; Kopczynska et al., 1986, 2001; Kang et al., 2001; Parslow et al., 2001; Smetacek et al., 2002; Kang et al., 2003; Kopczynska and Fiala, 2003; Fiala et al., 2004; Thomson et al., 2006; Kopczynska et al., 2007; Lange et al., 2015; Rigual-Hernández et al., 2015). Consequently, *Pseudo-nitzschia* can contribute significantly to the vertical flux of biological material, either as intact cells or within fecal pellets (Smith and Dunbar 1998; Accornero and Gowing 2003; Saggiomo et al., 2021). The toxins produced by some *Pseudo-nitzschia* species can enter the food web in several ways, potentially impacting marine life at multiple trophic levels.

Climate change models forecast increased average sea surface temperatures in Antarctic waters (IPCC, 2019). The IPCC (2019) presented a linkage between increasing temperatures and the occurrence of harmful algal blooms. *Pseudo-nitzschia* is an integral part of the phytoplankton community in the Southern Ocean, and experimental studies suggest that *Pseudo-nitzschia* in the Southern Ocean are well suited for dominating the phytoplankton community in a warmer ocean, in contrast to e.g. *Fragilariopsis*, another diatom genus of the central phytoplankton taxa (Jabre et al., 2021). Warmer Antarctic waters will, for example, benefit the growth of *P. subcurvata*, which has been shown to increase growth with temperatures and have maximum growth rates at 8 °C (Zhu et al., 2017). A potential shift in the phytoplankton community composition favoring *Pseudo-nitzschia* raises concerns regarding the production of domoic acid and its impacts on marine ecosystems, including marine mammals. While only a few Antarctic *Pseudo-nitzschia* strains have been examined for domoic acid production (Table 1), *P. subcurvata* has been confirmed to produce the toxin (Olesen et al., 2021). It is hypothesized that all *Pseudo-nitzschia* species may be able to produce DA under the right growth conditions (Lelong et al., 2012; Bates et al., 2018). Future research focusing on the genetic potential for domoic acid production (Brunson et al., 2018; Harðardóttir et al., 2019) could shed light on the prevalence of this trait. Given these factors, continuous research into the diversity, distribution, and toxicity of the *Pseudo-nitzschia* in the Southern Ocean is crucial for environmental and public health monitoring.

Dissolved domoic acid has been reported in the Southern Ocean at concentrations up to 220 ng L^{-1}, and moderately high quantities of cellular domoic acid reaching 0.85 ± 0.23 pg $cell^{-1}$ have been found in cells of *Pseudo-nitzschia* spp. (Silver et al., 2010; Geuer et al., 2019). Specifically, *P. subcurvata* has been found to contain lower quantities ranging from 3.09 to 7.28 10^{-5} pg domoic acid $cell^{-1}$ (Olesen et al., 2021). Otherwise, the few *Pseudo-nitzschia* species tested have been found non-toxic (present study, Fryxell et al., 1991, Kang et al., 1993). When interpreting toxin analyses, it should be taken into consideration that older studies likely used methods with less sensitivity compared to current standards (See also Table 1). It is also important to note that toxin production in non-toxic *Pseudo-nitzschia* can be induced by biotic factors such as copepod grazing (Harðardóttir et al., 2015), and that toxin production is known to vary immensely depending on chemical, physical and biological parameters (e.g. Lundholm et al., 2018). This potential for toxin production in *Pseudo-nitzschia* species, including those previously considered non-toxic, warrants continuous monitoring under varying environmental conditions.

To the best of our knowledge, domoic acid has not been found in higher trophic levels in the Southern Ocean, but in waters nearby, the toxin was found in high levels in four feces samples of the southern right whale *Eubalaena australis* (D'Agostino et al., 2017). Globally, domoic acid is known to cause both acute and chronic symptoms in marine mammals (Scholin et al., 2000; Goldstein et al., 2008; Rust et al., 2014; Cook et al., 2015;) and it can also impact other organisms in the food web like seabirds and copepods (Harðardóttir et al., 2018; Gibble et al., 2021; Olesen et al., 2022). Given the projected warming of the Southern Ocean, it is plausible to hypothesize the emergence of toxic diatom blooms with potentially severe impacts on marine life. It will therefore be essential to explore the toxic potential of the resident *Pseudo-nitzschia* species under different environmental conditions and whether more northern toxic species could be considered migrating south into a warmer Southern Ocean, as well as the presence of domoic acid in the Southern Ocean food web.

CRediT authorship contribution statement

Nina Lundholm: Writing – review & editing, Writing – original draft, Supervision, Investigation, Funding acquisition, Conceptualization. **Anneliese L. Christensen:** Writing – review & editing, Investigation. **Anna K.J. Olesen:** Writing – review & editing, Visualization, Investigation, Formal analysis. **Bánk Beszteri:** Writing – review & editing, Investigation. **Sarah Lena Eggers:** Writing – review & editing, Investigation. **Bernd Krock:** Writing – review & editing, Investigation. **Andreas Altenburger:** Writing – review & editing, Visualization, Investigation, Formal analysis.

Declaration of competing interest

The authors declare that they have no known competing financial interests or personal relationships that could have appeared to influence the work reported in this paper.

Data availability

Data will be made available on request.

Acknowledgements

We wish to thank Grethe Rytter Hasle† for provision of material and for valuable discussions, and Kira Holck Lundholm is thanked for scanning of micrographs. This work was funded by The Independent Research Fund Denmark through grant no 904000248B

Supplementary materials

Supplementary material associated with this article can be found, in the online version, at doi:10.1016/j.hal.2024.102724.

References

Accornero, A., Gowing, M.M., 2003. Annual sedimentation pattern of zooplankton fecal pellets in the Southern Ross Sea: what food webs and processes does the record imply? In: DiTullio, G.R., Dunbar, R.B. (Eds.), Biogeochemistry of the Ross Sea. American Geophysical Union, Washington, DC, USA, pp. 261–278.

Almandoz, G.O., Ferreyra, G.A., Schloss, I.R., Dogliotti, A.I., Rupolo, V., Paparazzo, F.E., Esteves, J.L., Ferrario, M.E., 2008. Distribution and ecology of *Pseudo-nitzschia* species (Bacillariophyceae) in the Weddell Sea (Antarctica) surface waters. Polar Biol. 31, 429–442.

Alvain, S., Moulin, C., Dandonneau, Y., Loisel, H., 2008. Seasonal distribution and succession of dominant phytoplankton groups in the global ocean: a satellite view.

Glob. Biogeochem. Cycles 22 (3), GB3001. https://doi.org/10.1029/2007GB003154.
Andreoli, C., Tolomio, C., Moro, I., Radice, M., Moschin, E., Bellato, S., 1995. Diatoms and dinoflagellates in Terra Nova Bay (Ross Sea-Antarctica) during austral summer 1990. Polar. Biol. 15, 465–475.
Armbrust, E., 2009. The life of diatoms in the world's oceans. Nature 459, 185–192. https://doi.org/10.1038/nature08057.
Arrigo, K.R., Robinson, D.H., Worthen, D.L., Dunbar, R.B., DiTullio, G.R., VanWoert, M., Lizotte, M.P., 1999. Phytoplankton community structure and the drawdown of nutrients and CO_2 in the Southern Ocean. Science (1979) 283 (5400), 365–367. https://doi.org/10.1126/science.283.5400.365.
Bates, S.S., Bird, C.J., Freitas, A.S.W., Foxall, R., Gilgan, M., Hanic, L.A., Johnson, J.R., Mcculloch, A.W., Odense, P., Pocklington, P., Quilliam, M.A., Sim, P.G., Smith, J.C., Subba Rao, D.V., Todd, E.C.D., Walter, J.A., Wright, J.L.C., 1989. Pennate diatom *Nitzschia pungens* as the primary source of domoic acid, a toxin in shellfish from eastern Prince Edward Island, Canand. Can. J. Fish. Aquat. Sci. 46, 1203–1215.
Bates, S.S., Hubbard, K.A., Lundholm, N., Montresor, M., Leaw, C.P., 2018. *Pseudo-nitzschia, Nitzschia*, and domoic acid: new research since 2011. Harmful Algae 79, 3–43. https://doi.org/10.1016/j.hal.2018.06.001.
Baustian, M.M., Bargu, S., Morrison, W., Sexton, C., Rabalais, N.N., 2018. The polychaete *Paraprionospio pinnata* is a likely vector of domoic acid to the benthic food web in the northern Gulf of Mexico. Harmful Algae 79, 44–49. https://doi.org/10.1016/j.hal.2018.06.002.
Brunson, J.K., McKinnie, S.M.K., Chekan, J.R., McCrow, J.P., Miles, Z.D., Bertrand, E.M., Bielinski, V.A., Luhavaya, H., Obornik, M., Smith, G.J., Hutchins, D.A., Allen, A.E., Moore, B.S., 2018. Biosynthesis of the neurotoxin domoic acid in a bloom-forming diatom. Science (1979) 361 (6409), 1356. https://doi.org/10.1126/science.aau0382.
Chen, X.M., Pang, J.X., Huang, C.x., Lundholm, N., Teng, S.T., Li, A., Li, Y., 2021. Two new and non-toxigenic *Pseudo-nitzschia* species (Bacillariophyceae) from Chinese southeast coastal waters. J. Phycol. 57, 335–344. https://doi.org/10.1111/jpy.13101-20-211.
Cleve, P.T., 1897. Report on the phyto-plankton collected on the expedition of H.M.S. 'Research,' 1896. Annual Report of the Fishery Board for Scotland, 15, 297-304, pl. VIII.
Cook, P.F., Reichmuth, C., Rouse, A.A., Libby, L.A., Dennison, S.E., Carmichael, O.T., Kruse-Elliott, K.T., Bloom, J., Singh, B., Fravel, V.A., Barbosa, L., Stuppino, J.J., Van Bonn, W.G., Gulland, F.M., Ranganath, C., 2015. Algal toxin impairs sea lion memory and hippocampal connectivity, with implications for strandings. Science (1979) 350 (6267), 1545–1547.
Costa, P.R., Mendes, C.R.B., Tavano, V.M., Dotto, T.S., Kerr, R., Monetiro, T., Odebrecht, C., Secchi, E.S., 2020. Dynamics of an intense diatom bloom in the Northern Antarctic Peninsula, February 2016. Limnol. Oceanogr. 65, 2056–2075.
Cremer, H., Roberts, D., McMinn, A., Gore, D., Melles, M., 2003. The holocene diatom flora of marine bays in the Windmill Islands, East Antarctica. Botanica Marina 46, 82–106.
D'Agostino, V.C., Degrati, M., Sastre, V., Santinelli, N., Krock, B., Krohn, T., Dans, S.L., Hoffmeyer, M.S., 2017. Domoic acid in a marine pelagic food web: exposure of southern right whales *Eubalaena australis* to domoic acid on the Peninsula Valdes calving ground, Argentina. Harmful Algae 68, 248–257.
Darty, K., Denise, A., Ponty, Y., 2009. VARNA: interactive drawing and editing of the RNA secondary structure. Bioinformatics. 25, 1974–1975.
David, B., Saucède, T., 2015. The southern ocean and its environment: a world of extremes. In: David, B., Saucède, T. (Eds.), Biodiversity of the Southern Ocean. Elsevier, pp. 17–31. https://doi.org/10.1016/B978-1-78548-047-8.50002-3.
Dong, H.C., Lundholm, N., Teng, S.T., Li, A., Wang, C., Hu, Y., Li, Y., 2020. Occurrence of the genus *Pseudo–nitzschia* and their domoic acid production in Guangdong coast, South China Sea. Harmful Algae 98, 101899.
Estrada, M., Delgado, M., 1990. Summer phytoplankton distributions in the Weddell Sea. Polar. Biol. 10, 441–449.
Fernandes, L.F., Hubbard, K.A., Richlen, M., Smith, J., Bates, S.S., Ehrman, J., Léger, C., Mafra Jr., L.L., Kulis, D., Quilliam, M., Erdner, D., Libera, K., McCauley, L., Anderson, D.M., 2014. Diversity and toxicity of the diatom *Pseudo-nitzschia* Peragallo in the Gulf of Maine, Northwestern Atlantic Ocean. Deep Sea Res. Part 2 Top Stud. Oceanogr. 103, 139–162.
Ferrario, M.E., Licea, S., 2006. Species of the genus *Pseudo-nitzschia* (Bacillariophyta) in Antarctic waters: morphology and distribution. Nov. Hed. Beih. 130, 1–16.
Ferrario, M., Licea, S., Balestrini, C.F., Ferreyra, G., 2004. Species of *Pseudo-nitzschia* in the Drake Passage (54°–61°S to 46°–64°W). In: Steidinger, K.A., Landsberg, J.H., Tomas, C.R., Vargo, G.A. (Eds.), Harmful Algae 2002. Florida Fish and Wildlife Conservation Commission, Florida Institute of Oceanography, and Intergovernmental Oceanographic Commission of UNESCO, pp. 434–436.
Fiala, M., Kopczyjska, E.E., Oriol, L., Machado, M.-C., 2004. Phytoplankton variability in the Crozet Basin frontal zone (Southwest Indian Ocean) during austral summer. J. Mar. Syst. 50, 243–261.
Fryxell, G.A., Kendrick, G.A., 1988. Austral spring microalgae across the Weddell Sea ice edge: spatial relationships found along a northward transect during AMERIEZ 83. Deep Sea Res. 35 (1), 1–20.
Fryxell, G.A., Garza, S.A., Roelke, D.L., 1991. Auxospore formation in an Antarctic clone of *Nitzschia subcurvata* Hasle. Diatom. Res. 6, 235–245.
Gai, F.F., Hedemand, C.K., Louw, D.C., Grobler, K., Krock, B., Moestrup, Ø., Lundholm, N., 2018. Morphological, molecular and toxigenic characteristics of Namibian *Pseudo-Nitzschia* species - including *Pseudo-nitzschia bucculenta* sp. nov. Harmful Algae 76, 80–95.
Garrison, D.L., Buck, K.R., Fryxell, G.A., 1987. Algal assemblages in Antarctic Pack ice and in ice-edge plankton. J. Phycol. 23, 564–572.
Garrison, D.L., Gibson, A., Kunze, H., Gowing, M.M., Vickers, C.L., Mathot, S., Bayre, R. C., 2003. The Ross Sea polynya project: diatom- and *Phaeocystis*-dominated phytoplankton assemblages in the Ross Sea, Antarctica, 1994–1996. In: Ditullio, G. R., Dunbar, R.B. (Eds.), Biogeochemistry of the Ross Sea, pp. 53–76. https://doi.org/10.1029/078ARS04.
Geuer, J.K., Krock, B., Leefmann, T., Koch, B.P., 2019. Quantification, extractability and stability of dissolved domoic acid within marine dissolved organic matter. Mar. Chem. 215, 103669.
Geuer, J.K., Trimborn, S., Koch, F., Brenneis, T., Krock, B., Koch, B.P., 2020. Dissolved domoic acid does not improve growth rates and iron content in iron-stressed *Pseudo-Nitzschia subcurvata*. Front. Mar. Sci. 7, 478.
Gibble, C.M., Kudela, R.M., Knowles, S., Bodenstein, B., Lefebvre, K.A., 2021. Domoic acid and saxitoxin in seabirds in the United States between 2007 and 2018. Harmful Algae 103, 101981.
Goldstein, T., Mazet, J.A., Zabka, T.S., Langlois, G., Colegrove, K.M., Silver, M., Bargu, S., Van Dolah, F., Leighfield, T., Conrad, P.A., Barakos, J., Williams, D.C., Dennison, S., Haulena, M., Gulland, F.M., 2008. Novel symptomatology and changing epidemiology of domoic acid toxicosis in California sea lions (*Zalophus californianus*): an increasing risk to marine mammal health. Proc. Biol. Sci. 275 (1632), 267–276.
Griffiths, H.J., 2010. Antarctic marine biodiversity – what do we know about the distribution of life in the Southern Ocean? PLoS ONE 5 (8), e11683. https://doi.org/10.1371/journal.pone.0011683.
Hamsher, S.E., Evans, K.M., Mann, D.G., Poulíčková, A., Saunders, G.W., 2011. Barcoding diatoms: exploring alternatives to COI-5P. Protist.Protist. 162 (3), 405–422. https://doi.org/10.1016/j.protis.2010.09.005.
Hansen, L.R., Soylu, S., Kotaki, Y., Moestrup, Ø., Lundholm, N., 2011. Toxin production and temperature-induced morphological variation of the diatom *Pseudo-nitzschia seriata* from the Arctic. Harmful Algae 10, 689–696.
Harðardóttir, S., Pančić, P., Tammilehto, A., Nielsen, T.G., Krock, B., Møller, E.F., Lundholm, N., 2015. Dangerous relations in the arctic marine food web – interactions between domoic acid producing *Pseudo-nitzschia* diatoms and *Calanus* copepodites. Mar Drugs 13, 3809–3835.
Harðardóttir, S., Krock, B., Wohlrab, S., Nielsen, T.G., John, U., Lundholm, N., 2018. Can domoic acid affect escape response in copepods? Harmful Algae 79, 50–52.
Harðardóttir, S., Wohlrab, S., Hjort, D.M., Krock, B., Nielsen, T.G., John, U., Lundholm, N., 2019. Transcriptomic responses to grazing reveal the metabolic pathway leading to the biosynthesis of domoic acid and highlight different defense strategies in diatoms. BMC Mol. Biol. 20 (1), 7. https://doi.org/10.1186/s12867-019-0124-0.
Hasle, G.R., 1964. *Nitzschia* and *Fragilariopsis* species studied in the light and electron microscopes. I. Some marine species of the groups *Nitzschiella* and *Lanceolatae*. Det Nor. Videnskaps-Akademi i Oslo, Mat.-Naturv. Klasse Ny serie 16, 1–48.
Hasle, G.R., 1965. *Nitzschia* and *Fragilariopsis* species studied in the light and electron microscopes. II. The group *Pseudonitzschia*. Skrifter Utgitt av Det Norske Videnskaps-Akademi i Oslo I. Mat.-Naturv. Klasse Ny serie 18, 1–45.
Hasle, G.R., 1969. An analysis of the phytoplankton of the Pacific Southern Ocean: abundance, composition and distribution during the Brategg expedition 1947/8. Hvalrådets Skrifter 52, 1–168.
Hasle, G.R., 1974. Validation of the names of some marine planktonic species of *Nitzschia* (Bacillariophyceae). Taxon.Taxon. 23, 425–428.
Hasle, G.R., 1994. *Pseudo-nitzschia* as a genus distinct from *Nitzschia* (Bacillariopyceae). J. Phycol. 30, 1036–1039.
Hasle, G.R., 1995. Nomenclatural notes on *Palmerina* nom. nov.: *Pseudo-Nitzschia turgiduloides* sp. nov. Diatom Research 10 (2), 357–358.
Hasle, G.R., 1993. Nomenclatural notes on marine planktonic diatoms. The family Bacillariaceae. In: P.A. Sims (Ed.), Progress in Diatom studies, Contributions to taxonomy, Ecology and nomenclature. Special volume in Honour of Robert Ross On the Occasion of His 80th Birthday. Beihefte zur Nova Hedwigia 106, 315–321.
Hasle, G.R., 2002. Are most of the domoic acid-producing species of the diatom genus *Pseudo-nitzschia* cosmopolites? Harmful Algae 1, 137–146.
Hasle, G.R., Medlin, L.K., 1990. Family Bacillariaceae: genus *Nitzschia*, Section *Pseudo-nitzschia* and section *Nitzschiella*. In: Medlin, L.K., Priddle, J. (Eds.), Polar Marine Diatoms. British Antarctic Survey, pp. 169–180.
Hasle, G.R., Syvertsen, E.E., 1997. Marine Diatoms. In: Tomas, C.R. (Ed.), Identifying Marine Phytoplankton. Academic, San Diego.
Hegseth, E.N., Von Quillfeldt, C.H., 2002. Low phytoplankton biomass and ice algal blooms in the Weddell Sea during the ice-filled summer of 1997. Antarctic Sci 14, 231–243.
Huang, C.X., Dong, H.C., Lundholm, N., Teng, S.T., Zheng, G.C., Tan, Z.J., Lim, P.T., Li, Y., 2019. Species composition and toxicity of the genus *Pseudo–nitzschia* in Taiwan Strait, including *P. chiniana* sp. nov. and *P. qiana* sp. nov. Harmful Algae 84, 195–209.
Huelsenbeck, J.P., Ronquist, F., 2001. MRBAYES: bayesian inference of phylogenetic trees. Bioinformatics. 17 (8), 754–755. https://www.ncbi.nlm.nih.gov/pubmed/11524383.
Hustedt, F., 1952. Diatomeen aus der Lebensgemeinschaft der Buckelwals (*Megaptera nodosa* Bonn.). Archiv für Hydrobiologie 46, 286–298.
Hustedt, F., 1958. Diatomeen aud der Antarktis und dem Südatlantik. Deutsche Antarktische Expedition 1938/39 II, 103–188.
IPCC, 2019. IPCC Special Report on the Ocean and Cryosphere in a Changing Climate. Cambridge University Press, Cambridge, UK and New York, NY, USA, pp. 755–pp. 10.1017/9781009157964.
Jabre, L.J., Allen, E.A., McCain, S.P., McCrow, J.P., Tenenbaum, N., Spackeen, J.L., Sipler, R.E., Green, B.R., Bronk, D.A., Hutchins, D.A., Bertrand, E.M., 2021. Molecular underpinnings and biogeochemical consequences of enhanced diatom

growth in a warming Southern Ocean. Proc. Natl. Acad. Sci. 118 (30), e2107238118. https://doi.org/10.1073/pnas.210723811.
Jensen, S.-K., Lacaze, J.-P., Hermann, G., Kershaw, J., Brownlow, A., Turner, A., Hall, A., 2015. Detection and effects of harmful algal toxins in Scottish harbour seals and potential links to population decline. Toxicon. 97, 1–14.
Kang, S.-H., Fryxell, G., 1993. Phytoplankton in the Weddell Sea, Antarctica: composition, abundance and distribution in water-column assemblages of the marginal ice-edge zone during austral autumn. Mar. Biol. 116 (2), 335–348.
Kang, S.-H., Kang, J.-S., Lee, S., Chung, K., Kim, D., Park, M., 2001. Antarctic Phytoplankton Assemblages in the marginal ice zone of the Northwestern Weddell Sea. J. Plankton Res. 23 (4), 333–352.
Kang, S.-H., Fryxell, G.A., Roelke, D.L., 1993. *Fragilariopsis cylindrus* (Grunow) Krieger compared with other species of the diatom family Bacillariaceae in Antarctic marginal ice edge zones. Nova Hedwigia, Beiheft 106, 335–352.
Kang, J.-S., Kang, S.-H., Kim, D., Kim, D.-Y., 2003. Planktonic centric diatom *Minidiscus chilensis* dominated sediment trap material in eastern Bransfield Strait, Antarctica. Mar. Ecol. Prog. Ser. 255, 93–99.
Kopczynska, E.E., Fiala, M., 2003. Surface phytoplankton composition and carbon biomass distribution in the Crozet Basin during austral summer of 1999: variability across frontal zones. Polar. Biol. 27, 17–28.
Kopczynska, E.E., Weber, L.H., El-Sayed, S.Z., 1986. Phytoplankton species composition and abundance in the Indian sector of the Antarctic Ocean. Polar. Biol. 6, 161–169.
Kopczynska, E.E., Dehairs, F., Elskens, M., Wright, S., 2001. Phytoplankton and microzooplankton variability between the Subtropical and Polar fronts south of Australia: thriving under regenerative and new production in late summer. J. Geophys. Res. 106 (C12), 31, 597–31,609.
Kopczynska, E.E., Savoye, N., Dehairs, F., Cardinal, D., Elskens, M., 2007. Spring phytoplankton assemblages in the Southern Ocean between Australia and Antarctica. Polar. Biol. 31, 77–88.
Krock, B., Tillmann, U., John, U., Cembella, A., 2008. LC-MS-MS aboard ship: tandem mass spectrometry in the search for phycotoxins and novel toxigenic plankton from the North Sea. Anal Bioanal Chem 392 (5), 797–803. https://doi.org/10.1007/s00216-008-2221-7.
Landan, G., Graur, D., 2008. Local reliability measures from sets of co-optimal multiple sequence alignments. Pac. Symp. Biocomput. 13, 15–24. https://www.ncbi.nlm.nih.gov/pubmed/18229673.
Lange, P.K., Tenenbaum, D.R., Tavano, V.M., Paranhos, R., Campos, L.S., 2015. Shifts in microphytoplankton species and cell size at Admiralty Bay, Antarctica. Antarct. Sci. 27 (3), 225–239.
Lefebvre, K.A., Quakenbush, L., Frame, E., Huntington, K.B., Sheffield, G., Stimmelmayr, R., Bryan, A., Kendrick, P., Ziel, H., Goldstein, T., Snyder, J.A., Gelatt, T., Gulland, F., Dickerson, B., Gill, V., 2016. Prevalence of algal toxins in Alaskan marine mammals foraging in a changing arctic and subarctic environment. Harmful Algae 55, 13–24.
Lelong, A., Hégaret, H., Soudant, P., Bates, S.S., 2012. *Pseudo-nitzschia* (Bacillariophyceae) species, domoic acid and amnesic shellfish poisoning: revisiting previous paradigms. Phycologia 51 (2), 168–216.
Lopes, V.M., Lopes, A.R., Costa, P., Rosa, R., 2013. Cephalopods as vectors of harmful algal bloom toxins in marine food webs. Mar. Drugs. 11 (9), 3381–3409. https://doi.org/10.3390/md11093381.
Lundholm, N., Daugbjerg, N., Moestrup, Ø., 2002. Phylogeny of the Bacillariaceae with emphasis on the genus *Pseudo-nitzschia* (Bacillariophyceae) based on partial LSU rDNA. Eur. J. Phycol. 37, 115–134.
Lundholm, N., Moestrup, Ø., Hasle, G.R., Hoef-Emden, K., 2003. A study of the *P. pseudodelicatissima/cuspidata*-complex (Bacillariophyceae). What is *Pseudo-nitzschia pseudodelicatissima* ? J. Phycol. 39, 797–813.
Lundholm, N., Moestrup, Ø., Kotaki, Y., Hoef-Emden, K., Scholin, C., Miller, P., 2006. Inter- and intraspecific variation of the *Pseudo-nitzschia delicatissima* complex (Bacillariophyceae) illustrated by rRNA probes, morphological data and phylogenetic analyses. J. Phycol. 42, 464–481.
Lundholm, N., Bates, S.S., Baugh, K.A., Bill, B.D., Connell, L.B., Léger, C., Trainer, V.L., 2012. Cryptic and pseudo-cryptic diversity in diatoms—With descriptions of *Pseudo-nitzschia hasleana* sp. nov. and *P. fryxelliana* sp. nov. J. Phycol. 48, 436–454.
Lundholm, N., Krock, B., John, U., Skov, J., Cheng, J., Pančić, M., Wohlrab, S., Rigby, K., Nielsen, T.G., Selander, E., Harðardóttir, S., 2018. Induction of domoic acid production in diatoms–Types of grazers and diatoms are important. Harmful Algae 79, 64–73.
Malviya, S., Scalco, E., Audic, S., Vincent, F., Veluchamy, A., Poulain, J., Wincker, P., Ludicone, D., de Vargas, C., Bittner, L., Zingone, A., Bowler, C., 2016. Insights into global diatom distribution and diversity in the world's ocean. Proc. Natl. Acad. Sci. U.S.A. 113, E1516–E1525.
Mangoni, O., Saggiomo, V., Bolinesi, F., Margiotta, F., Budillon, G., Cotroneo, Y., Misic, C., Rivaro, P., Saggiomo, M., 2017. Phytoplankton blooms during austral summer in the Ross Sea, Antarctica: driving factors and trophic implications. PLoS ONE 12 (4), e0176033. https://doi.org/10.1371/journal.pone.0176033.
Manguin, E., 1957. Premier inventaire des diatomées de la Terre Adélie Antarctique. Espèces nouvelles. Revue Algologique, Nouvelle Série 3, 111–134.
Manguin, E., 1960. Les diatomCes de la Terre AdBlie. Campagne du "Commandant Charcot" 1940-1950. Ann. Sci. Naturel. Bot. 12, 223–363.
Marchetti, A., Lundholm, N., Kotaki, Y., Hubbard, K., Harrison, P.J., Armbrust, E.V., 2008. Identification and assessment of domoic acid production in oceanic *Pseudo-nitzschia* (Bacillariophyceae) from iron-limited waters in the northeast subarctic Pacific. J. Phycol. 44, 650–661.
McCabe, R.M., Hickey, B.M., Kudela, R.M., Lefebvre, K.A., Adams, N.G., Bill, B.D., Gulland, F.M.D., Thomson, R.E., Cochlan, W.P., Trainer, V.L., 2016. An unprecedented coastwide toxic algal bloom linked to anomalous ocean conditions. Geophys. Res. Lett. 43, 10, 366–10,376.
McHuron, E.A., Greig, D.J., Colegrove, K.M., Fleetwood, M., Spraker, T.R., Gulland, F.M.D., Harvey, J.T., Lefebvre, K.A., Frame, E.R., 2013. Domoic acid exposure and associated clinical signs and histopathology in Pacific harbor seals (*Phoca vitulina richardii*). Harmful Algae 23, 28–33.
Nuccio, C., Innamorati, M., Lazzara, L., Mori, G., Massi, L., 2000. Spatial and temporal distribution of phytoplankton assemblages in the Ross Sea. In: Faranda, Guglielmo, Ionora (Eds.), Ross Sea Ecology. Springer Verlag, Berlin, pp. 231–245.
Olesen, A.J., Leithoff, A., Altenburger, A., Krock, B., Beszteri, B., Eggers, S.L., Lundholm, N., 2021. First evidence of the toxin domoic acid in Antarctic diatom species. Toxins. (Basel)Toxins. (Basel) 13, 93. https://doi.org/10.3390/toxins13020093.
Olesen, A.J., Ryderheim, F., Krock, B., Lundholm, N., Kiørboe, T., 2022. Costs and benefits of predator-induced defense in a toxic diatom. Proc. R. Soc. B. 289. https://doi.org/10.1098/rspb.2021.2735, 2021273520212735.
Parslow, J.S., Boyd, P.W., Rintoul, S.R., Griffiths, F.B., 2001. A persistent subsurface chlorophyll maximum in the Interpolar Frontal Zone south of Australia: seasonal progression and implications for phytoplankton-light-nutrient interactions. J. Geophys. Res. 106, 31543–31557. https://doi.org/10.1029/2000JC000322.
Petrou, K., Ralph, P.J., 2011. Photosynthesis and net primary productivity in three Antarctic diatoms: possible significance for their distribution in the Antarctic marine ecosystem. Mar. Ecol. Prog. Ser. 437, 27–40.
Reuter, J.S., Mathews, D.H., 2010. RNAstructure: software for RNA secondary structure prediction and analysis. BMC Bioinf 11, 129.
Riaux-Gobin, C., Poulin, M., Prodon, R., Treguer, P., 2003. Land-fast ice microalgal and phytoplanktonic communities (Adélie Land, Antarctica) in relation to environmental factors during ice break-up. Antarct. Sci. 15, 353–364. https://doi.org/10.1017/S0954102003001378.
Rigual-Hernández, A.S., Trull, T.W., Bray, S.G., Cortina, A., Armand, L.K., 2015. Latitudinal and temporal distributions of diatom populations in the pelagic waters of the Subantarctic and Polar Frontal Zones of the Southern Ocean and their role in the biological pump. Biogeosciences Discuss 12, 8615–8690.
Rousseaux, C., Gregg, W., 2014. Interannual variation in phytoplankton primary production at a global scale. Remote sens. (Basel) 6, 1–19.
Rust, L., Gulland, F., Frame, E., Lefebvre, K., 2014. Domoic acid in milk of free living California marine mammals indicates lactational exposure occurs. Mar. Mammal. Sci. 30 (3), 1272–1278.
Saggiomo, M., Escalera, L., Bolinesi, F., Rivaro, P., Saggiomo, V., Mangoni, O., 2021. Diatom diversity during two austral summers in the Ross Sea (Antarctica). Marine Micropal 165, 101993.
Schnetzer, A., Miller, P.E., Schaffner, R.A., Stauffer, B.A., Jones, B.H., Weisberg, S.B., DiGiacomo, P.M., Berelson, W.M., Caron, D.A., 2007. Blooms of *Pseudo-nitzschia* and domoic acid in the San Pedro Channel and Los Angeles harbor areas of the Southern California Bight, 2003–2004. Harmful Algae 6, 372–387.
Scholin, C.A., Gulland, F., Doucette, G.J., Benson, S., Busman, M., Chavez, F.P., Cordaro, J., DeLong, R., De Vogelaere, A., Harvey, J., Haulena, M., Lefebvre, K., Lipscomb, T., Loscutoff, S., Lowenstine, L.J., Marin 3rd, R., Miller, P.E., McLellan, W.A., Moeller, P.D., Powell, C.L., Rowles, T., Silvagni, P., Silver, M., Spraker, T., Trainer, V., Van Dolah, F.M., 2000. Mortality of sea lions along the central California coast linked to a toxic diatom bloom. Nature 403 (6765), 80–84.
Scott, F.J., Thomas, D.P., 2005. Diatoms. In: Scott, F.J., Marchant, H.J. (Eds.), Antarctic Marine Protists. Australian Biological Resources Study. Canberra and Australian Antarctic Division, Hobart, pp. 193–201.
Seibel, P.N., Muller, T., Dandekar, T., Schultz, J., Wolf, M., 2006. 4SALE–a tool for synchronous RNA sequence and secondary structure alignment and editing. BMC Bioinformatics 7 (1), 498.
Sela, I., Ashkenazy, H., Katoh, K., Pupko, T., 2015. GUIDANCE2: accurate detection of unreliable alignment regions accounting for the uncertainty of multiple parameters. Nucleic Acids Res. 43, W7–W14. https://doi.org/10.1093/nar/gkv318.
Silver, M.W., Bargu, S., Coale, S.L., Benitez-Nelson, C.R., Garcia, A.C., Roberts, K.J., Sekula-Wood, E., Bruland, K.W., Coale, K.H., 2010. Toxic diatoms and domoic acid in natural and iron enriched waters of the oceanic Pacific. Proc. Natl. Acad. Sci. U.S.A. 107, 20762–20767.
Simonsen, R., 1987. Atlas and catalogue of the diatom types of Friedrich Hustedt. Vol. 1 Catalogue X, 525 Vol. 2 Atlas, plates 1-395, Vol. 3 Atlas, plates 396-772, Cramer bei Borntraeger, Berlin und Stuttgart.
Smith Jr, W.O., Dunbar, R.B., 1998. The relationship between new production and vertical flux on the Ross Sea continental shelf. J. Mar. Syst. 17, 445–457. https://doi.org/10.1016/S0924-7963(98)00057-8.
Smetacek, V., Klaas, C., Menden-Deuer, S., Rynearson, T.A., 2002. Mesoscale distribution of dominant diatom species relative to the hydrographical field along the Antarctic Polar Front. Deep Sea Res. II 49, 3835–384.
Smith Jr, W.O., Ainley, D.G., Cattaneo-Vietti, R., 2007. Trophic interactions within the Ross Sea continental shelf ecosystem. Phil. Trans. R. Soc. B. 362, 95–111. https://doi.org/10.1098/rstb.2006.1956.
Stamatakis, A., 2014. RAxML version 8: a tool for phylogenetic analysis and post-analysis of large phylogenies. Bioinformatics. 30 (9), 1312–1313. https://doi.org/10.1093/bioinformatics/btu033.
Steyaert, J., 1973. Difference in diatom abundance between the two summer periods of 1965 and 1967 in Antarctic inshore waters (Breid Bay). Investigacion. Pesq. 37, 517–532.
Tammilehto, A., Nielsen, T.G., Krock, B., Møller, E.F., Lundholm, N., 2012. *Calanus* spp.—Vectors for the biotoxin, domoic acid, in the Arctic marine ecosystem? Harmful Algae 20, 165–174.

Teng, S.T., Lim, H.C., Lim, P.T., Dao, V.H., Bates, S.S., Leaw, C.P., 2014. *Pseudo-nitzschia kodamae* sp. nov. (Bacillariophyceae), a toxigenic species from the Strait of Malacca, Malaysia. Harmful Algae 34, 17–28.

Teng, S.T., Tan, S.N., Lim, H.C., Dao, V.H., Bates, S.S., Leaw, C.P., 2016. High diversity of *Pseudo-nitzschia* along the northern coast of Sarawak (Malaysian Borneo), with descriptions of *P. bipertita* sp. nov. and *P . limii* sp. nov. (Bacillariophyceae). J. Phycol. 52 (6), 973–989.

Thomson, P.G., McMinn, A., Kiessling, I., Watson, M., Goldsworthy, P.M., 2006. Composition and succession of dinoflagellates and chrysophytes in the upper fast ice of Davis Station, East Antarctica. Polar. Biol. 29, 337–345.

Trainer, V.L., Bates, S.S., Lundholm, N., Thessen, A.E., Cochlan, W.P., Adams, N.G., Trick, C.G., 2012. *Pseudo-nitzschia* physiological ecology, phylogeny, toxicity, monitoring and impacts on ecosystem health. Harmful Algae 14 (C), 271–300. https://doi.org/10.1016/j.hal.2011.10.025.

von Dassow, P., Mikhno, M., Percopo, I., Orellana, V.R., Aguilera, V., Alvarez, G., Araya, M., Cornejo-Guzman, S., Llona, T., Mardones, J.I., Norambuena, L., Salas-Rojas, V., Kooistra, W.H.C.F., Montresor, M., Sarno, D., 2023. Diversity and toxicity of the planktonic diatom genus *Pseudo-nitzschia* from coastal and offshore waters of the Southeast Pacific, including *Pseudo-nitzschia dampieri* sp. nov. Harmful Algae 130, 102520.

White, T.J., Bruns, T.D., Lee, S.B., Taylor, J.W., 1990. Amplification and direct sequencing of fungal ribosomal RNA Genes for phylogenetics. In: Innis, M.A., Gelfand, D.H., Sninsky, J.J., White, T.J. (Eds.), PCR Protocols: A Guide to Methods and Applications - A Laboratory Manual. Publisher, Academic Press, pp. 315–322.

WoRMS 2024. World Register of Marine Species https://www.marinespecies.org/aphia.php?p=taxdetails&id=149151.

Zhu, Z., Qu, P., Gale, J., Fu, F., Hutchins, D.A., 2017. Individual and interactive effects of warming and CO2 on *Pseudo-nitzschia subcurvata* and *Phaeocystis antarctica*, two dominant phytoplankton from the Ross Sea, Antarctica. Biogeosciences. 14, 5281–5295.